carrying an internal deletion of 30 amino acids in the cytoplasmic domain was found to incorporate dramatically reduced amounts of vRNP and M1 (14), implying that the cytoplasmic domain of BM2 might play an important role in viral assembly. On the other hand, for influenza A virus, truncation of the carboxy-terminal 28 amino acids from the cytoplasmic domain of the M2 protein greatly reduces virus infectivity and results in reduced incorporation of NP and viral RNA into virions (25). Similarly, truncation of the carboxy-terminal 22 amino acids from the M2 cytoplasmic domain reduces infectious virus titers and results in production of filamentous particles (16). A recent study identified the sequences of the M2 cytoplasmic domain that were required for specific incorporation of vRNP into virions and demonstrated interaction of the M2 cytoplasmic domain with the M1 protein (24).

To define in greater detail the role of the cytoplasmic domain in the assembly process, we generated a series of truncation and substitution mutants in the BM2 cytoplasmic domain using reverse genetics. The results showed that truncation of six amino acids from the carboxyl-terminal end of the BM2 protein affects the membrane association of M1 and greatly reduces incorporation of the vRNP complex into virions, resulting in altered particle morphology. We also found that amino acid substitutions within the carboxyl-terminal region result in a failure to incorporate the vRNP complex into virions. Given these findings, the cytoplasmic domain of BM2 protein may play key roles in the generation of infectious virus.

MATERIALS AND METHODS

Plasmids. The plasmid pCAGGS/BM2, which encodes the BM2 gene of B/Yamagata/1/73 (B/Yamagata) virus, has been described previously (32). To generate BM2 deletion constructs, the BM2 open reading frame was cloned into the pT7BlueBlunt vector (Novagen, Madison, WI) and the mutated BM2 genes were amplified by inverse PCR (primer sequences are available on request). PCR products were then cloned into the pCAGGS/MCS eukaryotic expression plasmid (31). The resulting constructs were designated pCBM2Δ104-109.

Cells and antibodies. MDCK cells were grown in Eagle's minimal essential medium supplemented with 10% fetal calf serum (FCS). Human embryonic kidney 293T cells and CK/BM2 cells (14) were cultured in Dulbecco's modified Eagle's medium containing 10% FCS. Stable cell lines expressing the wild-type or mutated BM2 protein were established as described previously (14). Briefly, MDCK cells were cotransfected with plasmid pCB7, encoding hygromycin resistance, and with the appropriate pCAGGS construct at a ratio of 3:1. Stable MDCK cell clones were selected in medium containing hygromycin at 0.2 mg/ml (Invitrogen, Carlsbad, CA) and were screened by an indirect immunofluorescence assay (IFA). Polyclonal anti-B/Yamagata virus antibodies have been described previously (32). A synthetic peptide, LSDNMERLSDHIVIEGLSAE, corresponding to amino acids 74 to 93 in the BM2 open reading frame of B/Yamagata virus, was synthesized by Bio-Synthesis (Lewisville, TX). For preparation of the antiserum specific for the influenza B virus BM2 protein, the peptide was coupled with keyhole limpet hemocyanin and mice were immunized. The antiactin antibody was obtained from Sigma (St. Louis, MO).

Reverse genetics. Plasmids to express mutant BM2 genes with truncations or substitutions were constructed as follows. Mutated M genes were amplified by PCR from pT7BlueBlunt containing the B/Yamagata M gene and were then digested using BsmBI (primer sequences provided on request). The BsmBI-digested fragment was cloned into the BsmBI sites of RNA expression polymerase I (Pol I) plasmids. All constructs were sequenced to ensure that no unwanted mutations were present. Transfectant influenza viruses were generated as described previously (14). Briefly, 293T cells (0.8 × 10⁶ cells) were plated the day before transfection. Twelve plasmids (eight Pol I constructs for eight RNA segments and four protein expression constructs for three polymerase proteins and NP) were mixed with transfection reagent (trans IT LT-1; Panvera, Madison, WI) at 2 μl/μg of DNA and then added to 293T cells in Dulbecco's modified Eagle's medium–10% FCS. At 16 h posttransfection, medium was replaced by Opti-MEM I (Invitrogen) containing 10 μg/ml of trypsin. At 48 h posttransfec-

tion, viruses in supernatants were collected and propagated in CK/BM2 cells in Opti-MEM I containing 10 μg/ml trypsin.

IFA. MDCK cells grown on coverslips were infected with wild-type and mutant viruses and incubated for 11 h at 34°C. Cells were washed three times with phosphate-buffered saline (PBS), fixed in 4% paraformaldehyde for 10 min at room temperature, and permeabilized with 0.1% Triton X-100 in PBS for 10 min. Background staining was blocked with 10% goat serum in PBS for 1 h. Cells were then incubated with anti-BM2 antibodies. After incubation for 1 h, cells were washed with PBS and incubated for 1 h with Alexa 488-conjugated goat anti-mouse immunoglobulin G (IgG) (Invitrogen). Coverslips were mounted on glass slides and examined using confocal microscopy (model LSM 510; Carl Zeiss, Oberkochen, Germany).

Western blotting. MDCK cells were infected with virus at a multiplicity of infection (MOI) of 10 PFU/cell and incubated at 34°C. At 10 h postinfection (p.i.), cells were lysed in radioimmunoprecipitation assay buffer (50 mM Tris-HCl [pH 8.0], 150 mM NaCl, 1% NP-40, 0.5% deoxycholate, and 0.1% sodium dodecyl sulfate [SDS]) and maintained for 30 min on ice. After clarification by centrifugation, the supernatant was dissolved in SDS sample buffer (50 mM Tris-HCl [pH 6.8], 5% 2-mercaptoethanol, 2% SDS, 10% glycerol, and bromophenol blue) at 95°C for 5 min, resolved by SDS-polyacrylamide gel electrophoresis (PAGE), and electroblotted to Immobilon-P paper (Millipore, Billerica, MA). After incubation with the appropriate antibody (antiserum to BM2 or B/Yamagata virion), the membrane was treated with horseradish peroxidase-conjugated anti-mouse IgG for influenza B virus BM2 or HRP-conjugated anti-rabbit IgG for B/Yamagata virion, respectively, and visualized by enhanced chemiluminescence according to protocols provided by GE Healthcare Life Sciences (Little Chalfont, England). Band intensities were measured with a LightCapture system (model AE-6961; ATTO, Tokyo, Japan) using a CS analyzer (ATTO).

Analysis of the protein composition of virions. MDCK cells grown in 10-cm dishes were infected with wild-type or mutant virus at an MOI of 5 PFU and cultured in Opti-MEM I at 34°C. At 24 h p.i., supernatants from cell culture were harvested and clarified by centrifugation at 1,620 × g for 10 min at 4°C. Virions were purified by centrifugation through 30% sucrose in a SW41 Ti rotor (Beckman Coulter, Fullerton, CA) at 150,000 × g for 1 h at 4°C. Pellets were then suspended in 50 mM Tris-HCl (pH 7.5), and the samples were analyzed by SDS-PAGE. Proteins were detected by using Coomassie brilliant blue and Western blotting using anti-BM2 antibody. The profiles of the stained gels were digitized and were quantified as described previously (14).

Real-time PCR. RNA was extracted from purified virions using an RNeasy kit (Qiagen, Hilden, Germany) in accordance with the instructions of the manufacturer. The cDNAs were synthesized by reverse transcription of vRNA with an oligonucleotide complementary to the conserved 3' end of vRNA. Primer and probe sequences for B/Yamagata virus HA genes have been described previously (14). Amplification and detection by real-time PCR were performed using the Chromo-4 real-time PCR detection system (Bio-Rad, Hercules, CA). PCR was performed with 50 μl of reaction mixture consisting of 1× PCR buffer (GeneAmp Gold PCR reagent kit; Applied Biosystems, Foster City, CA), 250 μM of each deoxynucleoside triphosphate, 5 mM MgCl₂, 1.25 U of AmpliTaq Gold DNA polymerase (Applied Biosystems), 0.2 μM each of forward and reverse primers, 0.1 μM of probe, and 5 μl of cDNA. Reaction conditions were set at 50°C for 2 min and 95°C for 10 min, followed by 40 cycles of 95°C for 15 s and 60°C for 1 min. The standard curve for this assay was calculated using a series of 10-fold dilutions of Pol I plasmids encoding the B/Yamagata virus HA gene.

Protease treatment of virions. Purified virions in 50 mM Tris-HCl (pH 7.5) were digested with 0.05 mg/ml trypsin (sequencing grade; Roche, Mannheim, Germany) at 25°C. After incubation for 2 h, digestion was stopped by adding 4-(2-aminoethyl)-benzenesulfonyl fluoride (Roche) to a 4 mM concentration. Samples were dissolved in SDS sample buffer and subjected to SDS-PAGE.

Electron microscopy. A droplet of purified virions was placed on a 400-mesh copper grid (Veco, Eiersbeck, The Netherlands) coated with collodion and then negatively stained with 1% uranylacetate. Images were obtained using an H-7000 transmission electron microscope (Hitachi, Tokyo, Japan) operated at 75 kV.

Flotation analysis. Flotation analysis was performed as described previously with modifications (21). Briefly, virus-infected cells were washed and scraped into PBS containing 0.9 mM CaCl₂ and 0.49 mM MgCl₂. Cells were pelleted by centrifugation for 2 min at 500 × g and resuspended in 1.2 ml of lysis buffer (20 mM Tris-HCl [pH 8.0], 250 mM sucrose, 1 mM MgCl₂, and 1 mM CaCl₂) containing protease inhibitors at final concentrations of 1.04 mM aminoethylbenzene sulfonyl fluoride, 0.8 μM aprotinin, 20 μM leupeptin, 40 μM bestatin, 15 μM pepstatin A, and 14 μM E-64. Cells were then disrupted by repeated passage (40 times) through a 22-gauge needle. Unbroken cells and nuclei were

FIG. 1. Schematic diagram of wild-type and mutant BM2 proteins carrying a carboxyl-terminal truncation in the BM2 cytoplasmic domain. Amino acid sequence of the BM2 cytoplasmic domain (residues 90 to 109) is shown. The asterisk indicates a stop codon.

removed by centrifugation at 1,000 × g for 10 min at 4°C. Postnuclear superna-tants (1.2 ml) were dispersed into 1.2 ml of 60% (wt/wt) OptiPrep (AXIS-SHIELD PoC AS, Oslo, Norway) in 20 mM Tris-HCl (pH 8.0) plus protease inhibitors, placed at the bottom of the tube, and then overlaid with a gradient series of 25%, 20%, 15%, and 10% OptiPrep layers containing 20 mM Tris-HCl (pH 8.0), 125 mM sucrose, 1 mM MgCl2, 1 mM CaCl2, and protease inhibitors. The gradient was centrifuged for 14 h at 59,200 × g using an SW-55Ti rotor in a Beckman ultracentrifuge. Samples (400 µl) of the gradient were collected from bottom to top and directly subjected to SDS-PAGE.

RESULTS

Generation of influenza B virus mutants carrying the truncated cytoplasmic domain of the BM2 protein by reverse genetics. To explore the functional role of the cytoplasmic domain of the BM2 protein in the replication cycle of influenza B virus, we constructed cDNAs encoding BM2 proteins with the cytoplasmic domain truncated at three (BM2Δ107-109), six (BM2Δ104-109), or nine (BM2Δ101-109) amino acids from the carboxyl-terminal end (Fig. 1). Influenza B viruses possessing these truncated BM2 proteins were generated by reverse genetics based on the backbone of B/Yamagata virus genes using eight Pol I plasmids encoding genomic RNAs and four protein expression plasmids (PB1, PB2, PA, and NP) as described previously (14). The resultant BM2Δ107-109 mutant was obtained with efficiency as high as that of the wild-type virus (rg-B/Y wt) from plasmid-transfected 293T cells, whereas the other two mutants, the BM2Δ104-109 and BM2Δ101-109 mutants, were not rescued (data not shown). These 2 mutants were recovered when our 12-plasmid system was supplemented with the wild-type BM2 expression plasmid as mentioned above. Rescued mutants in the culture supernatant were then amplified in the MDCK cell line, CK/BM2, which is able to constitutively express the wild-type BM2 protein for preparation of working stock viruses. Titers of virus stocks were determined by a plaque assay with CK/BM2 cells, and all mutants showed titers similar to that of rg-B/Y wt ($\sim 1 \times 10^8$ PFU/ml). By sequencing RNA segment 7 of recovered mutants, we confirmed no reversion and no additional mutations in the segment.

Synthesis and localization of BM2 proteins in cells infected with BM2 deletion mutants. To examine whether BM2 protein expression was affected by truncation of the cytoplasmic domain, MDCK cells were infected with mutants and synthesis of the truncated BM2 proteins was analyzed by Western blotting using anti-BM2 antibody. All truncated BM2 proteins were found with the expected molecular sizes, although migration

ratios of the BM2Δ104-109 and BM2Δ101-109 proteins did not differ significantly from each other (Fig. 2A). Expression levels of mutant proteins were estimated using a CS analyzer as described in Materials and Methods. The BM2Δ107-109 protein was expressed at levels equivalent to that of the wild-type BM2 protein, whereas BM2Δ104-109 and BM2Δ101-109 showed lower expression levels of 57% and 54%, respectively. These differences were not reflected in the efficacy of virus recovery and growth, as shown below.

FIG. 2. Detection of the BM2 protein in BM2 truncation mutant virus-infected MDCK cells. (A) MDCK cells were infected with rg-B/Y wt and BM2stop viruses. At 10 h p.i., the BM2 protein in cell lysates was detected by Western blotting using anti-BM2 antibody. Quantitation of BM2 proteins was performed using an ATTO CS analyzer, and percentages were determined relative to values obtained for the wild-type BM2 protein. (B) At 11 h p.i., infected cells were fixed and stained for indirect immunofluorescence using anti-BM2 antibody.
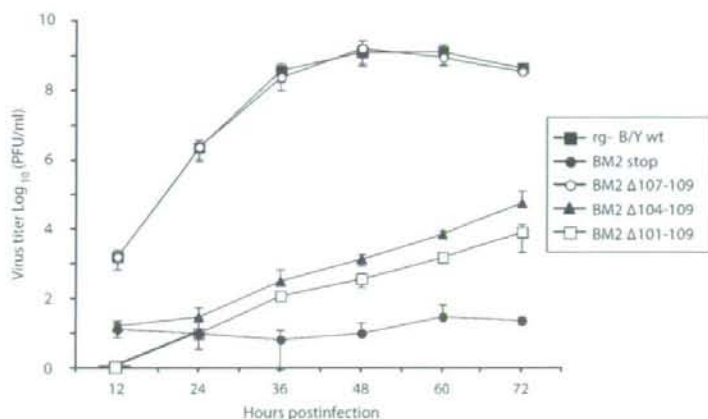
FIG. 3. Growth properties of BM2 truncation mutant viruses. MDCK cells were infected at an MOI of 0.001 PFU, and supernatants of infected cells were harvested at the indicated times. Titer of virus in the supernatant was determined by a plaque assay on CK/BM2 cells.

The BM2 protein is transported to the plasma membrane through the trans-Golgi network (47). To determine whether truncation in the cytoplasmic domain of the BM2 protein results in a failure of proper transport to the plasma membrane, localization of truncated BM2 proteins in mutant-infected MDCK cells was examined by IFA using anti-BM2 antibody (Fig. 2B). Truncated BM2 proteins were detected along the plasma membrane and at the Golgi apparatus of infected cells, and localization profiles were indistinguishable from that of the wild-type BM2 protein, indicating that truncation of nine amino acids from the carboxyl-terminal end of the BM2 protein does not significantly affect BM2 protein transport to the plasma membrane.

Growth properties of BM2 mutants in MDCK cells. We compared the kinetics of virus production in a multiple-step growth cycle among BM2 truncation mutants. MDCK cells were infected with virus at an MOI of 0.001, and titers of virus in the supernatant were measured by a plaque assay with CK/BM2 cells. rg-B/Y wt and the BM2 knockout mutant (BM2stop; see reference 14) were included for comparison of the growth properties of mutants. The BM2Δ107-109 mutant was indistinguishable in terms of both growth kinetics and maximum yield from rg-B/Y wt virus (Fig. 3). However, growth of the BM2Δ104-109 and BM2Δ101-109 mutants was extremely low, and the yield at 36 h p.i. was approximately 6 logs less than that of rg-B/Y wt, although growth was better than that of the BM2stop mutant. These results indicate that truncation of six or more amino acids at the carboxyl-terminal end caused great suppression of infectious virus production.

Viral components in the virion of BM2 mutant viruses. We have previously demonstrated using the BM2stop mutant that a lack of the BM2 protein severely blocks incorporation of vRNP complex into the virion (14). To determine whether truncation of the BM2 cytoplasmic domain affects incorporation of vRNP complex that can be traced by detection of the NP protein and a representative vRNA segment in the virion, MDCK cells were infected with mutant viruses at an MOI of 5 for 24 h. Progeny viruses released into the culture supernatant were purified and analyzed by SDS-PAGE followed by Coo-

massie brilliant blue staining (Fig. 4A). Components of purified virions of mutants were compared with those of rg-B/Y wt and BM2stop viruses. In the virion of BM2Δ107-109 virus, which replicated normally (Fig. 3), the NP protein was incorporated at levels similar to those for rg-B/Y wt virus when total virion protein was normalized with the HA protein (Fig. 4B). In contrast, for BM2Δ104-109 and BM2Δ101-109 virions, mutants grew very poorly (Fig. 3) and incorporation of the NP protein into virions was dramatically decreased, to levels similar to that for the BM2stop mutant, although each of the truncated BM2 proteins was incorporated into the particles (Fig. 4B). Moreover, amounts of M1 proteins in the BM2Δ104-109 and BM2Δ101-109 mutants were found to be 67% and 27%, respectively, of those in rg-B/Y wt virus. To determine the relative amounts of vRNA incorporation into BM2 mutant virions, vRNA was extracted from purified virions and copy numbers of the HA gene as a representation of vRNA segments were quantified by real-time reverse transcription-PCR using HA gene-specific primers as previously described (14). Incorporation of vRNA of the BM2Δ107-109 mutant was detected to be at a similar level to that of rgB/Y wt, whereas vRNA levels of the BM2Δ104-109 and BM2Δ101-109 mutants were 1/3 and 1/5 of levels for rgB/Y wt, respectively (Fig. 4C). Taken together, these results suggest that deletion of six amino acids from the carboxyl-terminal end of the BM2 protein gives rise to a marked decrease in vRNP complex incorporation in the virion assembly process, so that production of infectious particles is extremely suppressed.

We also observed that BM2stop, BM2Δ104-109, and BM2Δ101-109 virions contained increased amounts of nonviral proteins (Fig. 4A). However, proteins detected with virions of mutants may have represented contaminants attached to the virion surface and/or cell membrane fragments. To explore this, virions were treated with trypsin in the presence or absence of 1% Triton X-100 and then analyzed by Coomassie brilliant blue staining (Fig. 4D, upper panel). A 44-kDa polypeptide was still detected in virions even after trypsin treatment, as were the internal virion proteins NP and M1 (Fig. 4D, lanes 4, 8, and 10), but not after treatment in the
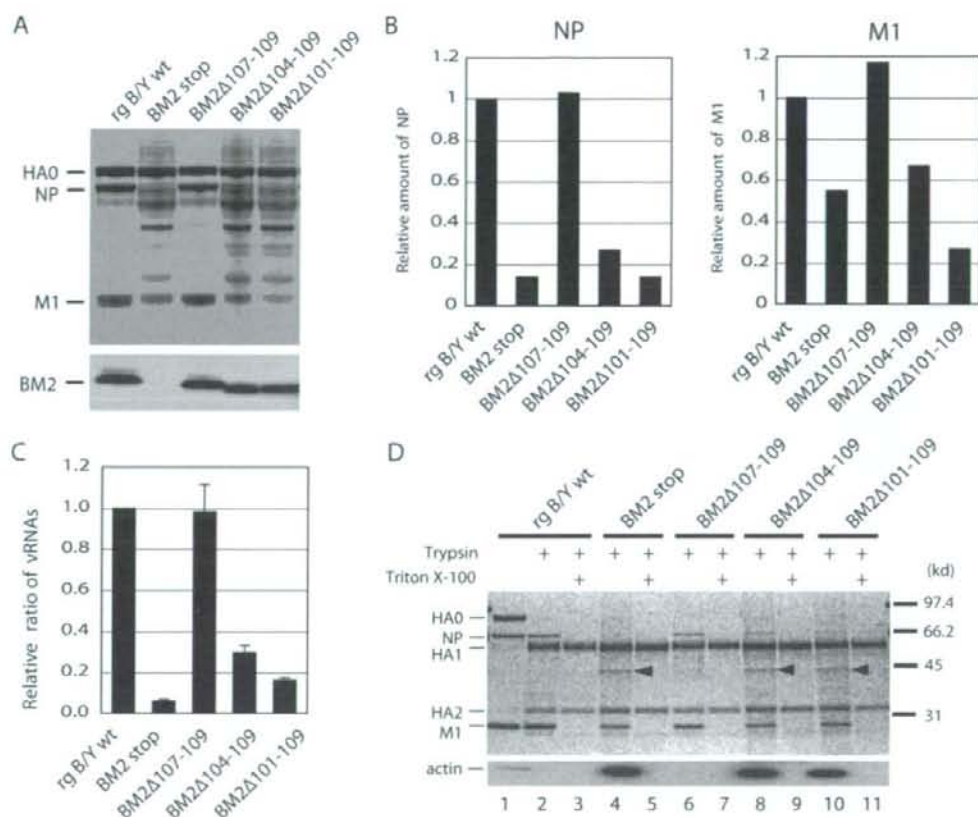
FIG. 4. Viral proteins and RNA segments in BM2 mutant virus particles. MDCK cells were infected at an MOI of 5 PFU, and virions were purified by centrifugation through 30% sucrose. (A) Protein composition of BM2 mutant and rg-B/Y wt virions. Purified virions produced by MDCK cells were analyzed by Coomassie brilliant blue staining (upper panel) and Western blotting using anti-BM2 antibody (lower panel). (B) Relative amounts of viral proteins. Viral proteins were quantified using an ATTO CS analyzer, and relative staining intensity of each protein was normalized to that of HA for each virus. (C) Relative ratio of HA genes between BM2 mutant and rg-B/Y wt virions. RNA was extracted from virions grown in MDCK cells and reverse transcribed, and the resultant cDNA was quantified using real-time PCR with primers directed to HA genes (see Materials and Methods). Mutant virions analyzed contained amounts of the HA protein equal to those of rgB/Y wt virions. All samples were run in duplicate and repeated three times. Error bars represent standard errors of the mean. (D) Analysis of proteins in protease-treated virions. Purified virions were incubated at 25°C with 0.05 mg/ml trypsin in the absence or presence of 1% Triton X-100. AEBSF was then added to 4 mM, and each sample was analyzed by Coomassie brilliant blue staining (upper panel) and by Western blotting using antiactin antibody (lower panel). Arrowheads indicate cellular actin. Mobilities of molecular mass markers are shown on the right.

presence of Triton X-100 (Fig. 4D, lanes 5, 9, and 11), indicating that the 44-kDa polypetide was incorporated into virions together with viral components. Influenza A virus viruses are known to incorporate cellular actin into virions (39), and this protein has a molecular mass of 42 kDa. As a result, we next examined whether the 44-kDa polypeptide really represented actin by Western blotting analysis using antiactin antibody. The data indicated that BM2stop, BM2Δ104-109, and BM2Δ101-109 virions contained increased amounts of actin (Fig. 4D, lower panel). Taken together, these data suggest that exclusion of actin from progeny virions is affected by truncations in the cytoplasmic domain of the BM2 protein.

Analysis of virions by electron microscopy. Previous studies of influenza A virus have shown that deletion of the cytoplasmic domains of the HA and NA glycoproteins and the M1

protein affects the size and shape of the virus particle, often resulting in formation of long filamentous structures (16, 17, 27). To determine whether the lack of BM2 and truncation of the BM2 cytoplasmic domain alters normal morphogenesis in B/Yamagata virus particles, MDCK cells were infected with mutant viruses at an MOI of 5 for 24 h and virions were purified and examined by negative-staining electron microscopy (Fig. 5). BM2Δ107-109 virions displayed a typical uniform spherical shape with a diameter similar to that of rg-B/Y wt virions (Fig. 5). However, BM2Δ104-109, BM2Δ101-109, and BM2stop virions were enlarged and either spherical or amorphous (Fig. 5). These results suggest that the failure of vRNP complex and M1 incorporation caused by the truncation or lack of the BM2 protein exerts profound effects on virion morphogenesis.

rg B/Y wt

BM2 stop

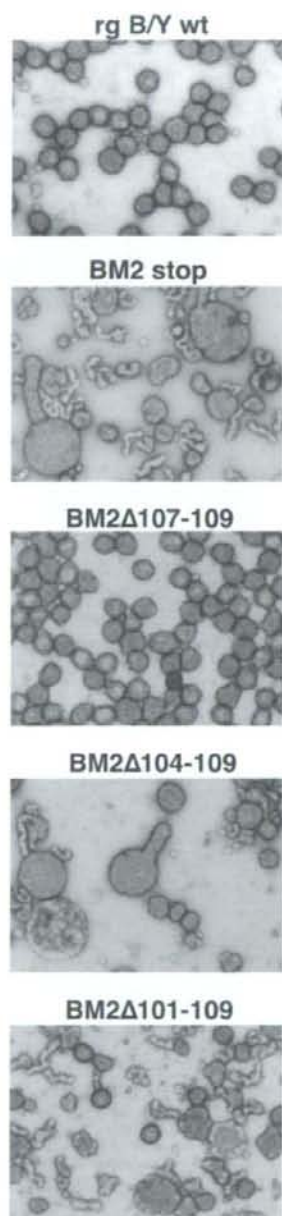**BM2Δ107-109**

BM2Δ104-109

BM2Δ101-109

FIG. 5. Morphologies of mutants observed by using negative-staining electron microscopy. Virions were grown in MDCK cells and purified by centrifugation through 30% sucrose. Virions were negatively stained with 1% uranylacetate and observed by using transmission electron microscopy. Bar, 200 nm.

Truncated BM2 protein does not support intact infectious virus production. Since deletion of six amino acids from the carboxyl-terminal end of the BM2 protein was not tolerated for normal virion assembly or production of infectious virus, we

focused on the BM2Δ104-109 mutant for further characterization of the BM2 protein in the present study. BM2 knockout virus was able to grow normally when the wild-type BM2 protein was supplemented in *trans* by host cells expressing BM2 (14). We therefore examined whether growth of BM2 knockout virus could be regained by *trans* supplementation of the truncated BM2 protein. To this end, the growth properties of rg-B/Y wt, BM2stop, and BM2Δ104-109 viruses were examined in a cell line expressing wild-type BM2 or BM2Δ104-109. In the presence of supplemental wild-type BM2 protein, growth of BM2stop and BM2Δ104-109 viruses was restored to levels similar to that seen for rg-B/Y wt virus (Fig. 6A). The resulting virion also contained amounts of NP and M1 proteins comparable to those in rg-B/Y wt virus (Fig. 6B, lanes 2 and 3). Conversely, *trans* supplementation of the BM2Δ104-109 protein did not accelerate the growth of BM2stop and BM2Δ104-109 viruses (Fig. 6A), and virions failed to incorporate vRNP complex, although the truncated BM2 protein was incorporated into virions (Fig. 6B, lanes 5 and 6). These findings support the notion that the cytoplasmic domain of the BM2 protein plays a substantial role in packaging of vRNP complex during the assembly process and in the production of infectious virus.

Membrane association of M1 was greatly suppressed in the presence of the truncated BM2 protein. We have previously reported that BM2 increases the membrane association of M1 (14). To test whether truncation of the carboxyl-terminal region of BM2 alters the membrane association of M1, virus-infected cells at 11 h p.i. were examined by iodixanol flotation centrifugation analysis followed by Western blotting using anti-B/Yamagata and anti-BM2 antibodies. In this experiment, the majority of membrane sedimented in fractions 6 to 10. In cells infected with rg-B/Y wt, the majority of M1 (74%) sedimented in membrane fractions together with the integral transmembrane proteins, HA and BM2 (Fig. 7A, B, and D, upper row of each panel). In cells infected with the BM2Δ104-109 mutant, on the other hand, only small amounts of M1 floated up with membranes while the majority (71%) remained in fractions 1 to 5, containing the majority of soluble NP, although distributions of HA, NP, and BM2 resembled those of rg-B/Y wt (Fig. 7). Those distribution profiles were essentially identical to that of the BM2stop mutant. These results strongly suggest that the membrane association of M1 was affected by the six-amino-acid truncation of the carboxyl-terminal end of BM2, resulting in a failure to package vRNP complex into virions.

Characterization of influenza B virus mutants with alanine substitutions in the cytoplasmic domain. Since truncation of the carboxyl-terminal end of the BM2 protein affected normal incorporation of vRNP complex into virions (Fig. 4), this region can be postulated to contain an effector domain of the BM2 protein. To address this issue, we generated a series of alanine-scanning substitution mutants encoding a BM2 protein with a block of three adjacent amino acids changed to alanine, spanning amino acids 86 to 109 (Fig. 8), and amplified the mutants using the same methods used for recovery of the BM2 deletion mutant. Growth properties of these mutants in MDCK cells are shown in Fig. 9A. The BM2 104-106A and BM2 107-109A mutant viruses exhibited growth kinetics indistinguishable from that of rg-B/Y wt virus. The BM2 98-100A and BM2 101-103A mutants revealed slightly delayed virus
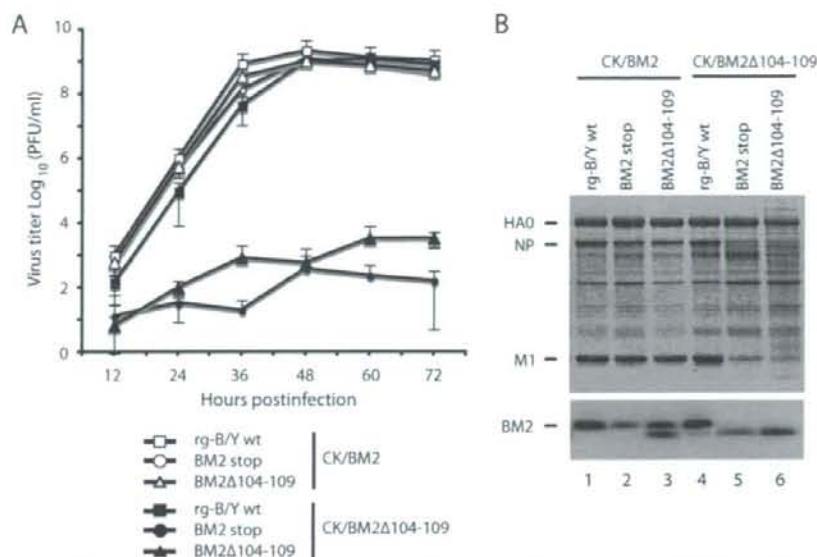
FIG. 6. The BM2Δ104-109 mutant protein did not support intact infectious virus production. (A) Multiple-step growth curve of rg-B/Y wt, BM2stop, and BM2Δ104-109 viruses. CK/BM2 and CK/BM2Δ104-109 cells were infected at an MOI of 0.001 PFU, and supernatants of infected cells were harvested at the indicated times. Titer of virus in the supernatant was determined by a plaque assay on CK/BM2 cells. (B) Protein composition of rg-B/Y wt, BM2stop, and BM2Δ104-109 virions was analyzed by Coomassie brilliant blue staining (upper panel) and Western blotting using anti-BM2 antibody (lower panel).

production but reached titers similar to that of rg-B/Y wt virus at 60 h p.i. In contrast, BM2 89-91A, BM2 93-94A, and BM2 95-97A mutants did not display substantial growth, similar to the BM2stop mutant, and titers at 60 h p.i. were approximately 6 logs lower than that of rg-B/Y wt virus. Virions of these mutants, as expected, contained significantly reduced levels of NP and M1, although substitution BM2 mutant proteins were incorporated into the particles (Fig. 9B). The mutant BM2 86-88A had a titer higher than that of the BM2stop, BM2 89-91A, BM2 93-94A, and BM2 95-97A mutants but definitely lower than those of the rest of the mutants and rg-B/Y wt. Virus particles for this mutant also contained smaller amounts of NP. When the amounts of the HA protein from purified BM2stop, BM2 86-88A, BM2 89-91A, BM2 93-94A, and BM2 95-97A mutants were normalized, the amount of the NP protein in BM2 86-88A virions was 1.3- to 2.5-fold larger than those of the others (data not shown). This slight increase in NP incorporation in BM2 86-88A virions is likely to reflect an increase in virus production. These results indicate that 12 amino acids of the carboxyl terminus are variable but the adjacent upstream 12 amino acids are required for efficient assembly of vRNP complex into the virion.

DISCUSSION

The influenza B virus BM2 protein has the longest cytoplasmic domain of the various influenza virus integral membrane proteins. Previous studies using reverse-genetics techniques for influenza B virus have shown that viruses encoding BM2 proteins with large deletions in the cytoplasmic domain do not grow substantially in cell culture and produce progeny viruses

lacking vRNP complex (14), suggesting that the BM2 cytoplasmic domain might play an important role during the life cycle of influenza B virus.

To further explore the role of the long cytoplasmic domain of BM2 in the life cycle of influenza B virus, we generated and characterized the phenotypes of influenza B viruses bearing deletions or alanine substitutions within the BM2 cytoplasmic domain. Influenza B viruses encoding the BM2 protein with a six-residue (BM2Δ104-109) or nine-residue (BM2Δ101-109) deletion at the carboxyl terminus produced viruses containing dramatically reduced vRNP complex, as seen with BM2 knockout mutants, although intracellular transport was indistinguishable from that of the wild-type BM2 protein and incorporation into virus particles was achieved. Similarly, dramatic reductions of NP incorporation were also observed for virus particles of BM2 mutants (BM2 86-88A, BM2 89-91A, BM2 93-94A, and BM2 95-97A) with three consecutive alanine substitutions in the region from position 86 to 97. These data were further supported by observations that BM2 knockout virus was able to replicate successfully in cell culture by *trans* supplementation of the wild-type BM2 protein but not by *trans* supplementation of the truncated BM2 protein. Taken together, these findings indicate that the cytoplasmic domain of BM2 plays a crucial role for production of infectious virus particles. Similar evidence has recently been obtained for influenza A virus, where efficient production of infectious virus depends on the presence of the cytoplasmic domain of the M2 protein (16, 25).

BM2 and influenza A virus M2 have been shown to possess similar H⁺ ion channel activity (36). The ion channel is considered necessary for efficient vRNP uncoating during viral
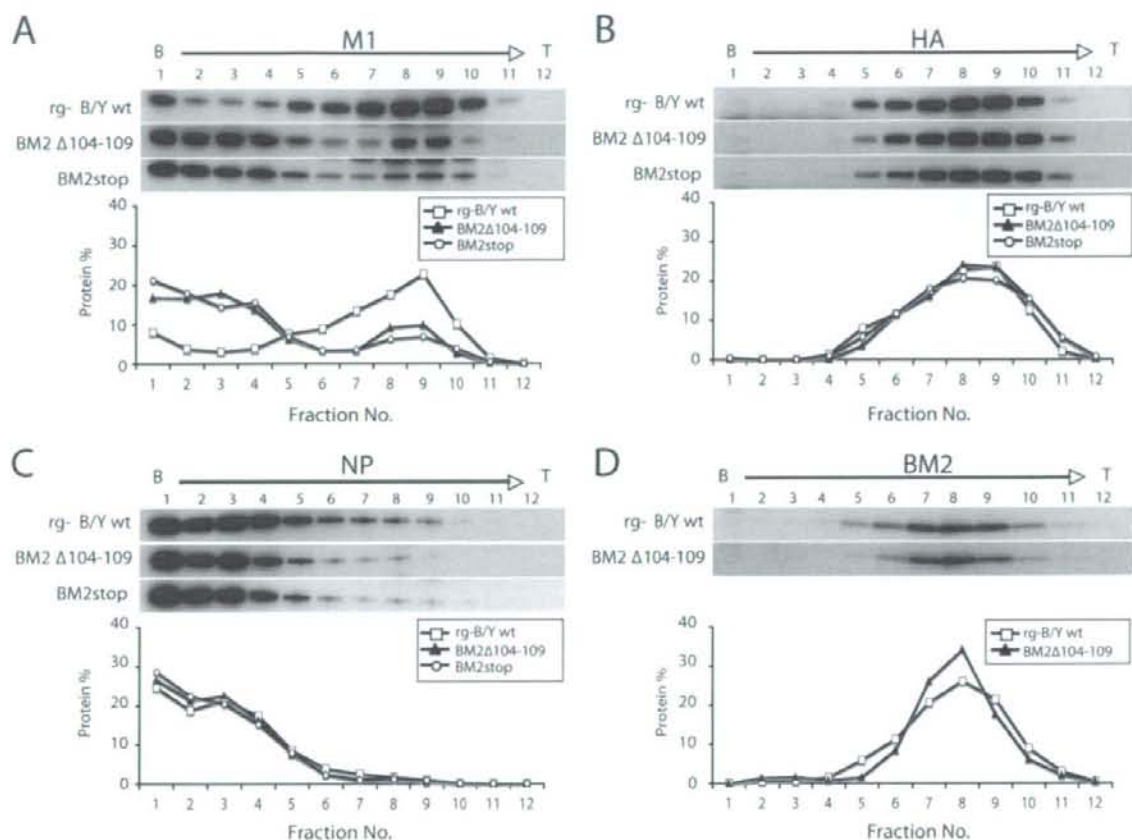
FIG. 7. Membrane association of viral proteins in virus-infected cells. MDCK cells were infected with rg-B/Y wt, BM2Δ104-109, and BM2stop viruses. At 11 h p.i., infected cells were lysed and postnuclear fractions were subjected to equilibrium centrifugation as described in Materials and Methods. M1 (A), HA (B), NP (C), and BM2 (D) proteins in all fractions collected from top (T) to bottom (B) were analyzed by Western blotting using anti-B/Yamagata and anti-BM2 antibodies (upper panels). Viral proteins were quantified using an ATTO CS analyzer. The amount of viral protein in each fraction is expressed as a percentage of the total amount in all fractions (lower panels).

entry (13). The transmembrane domain of influenza A virus M2 and influenza B virus BM2 contains consensus peptide motifs (19-HXXXW-23) involved in ion channel activity. Electrophysiological studies of BM2 in *Xenopus* oocytes and mammalian cells have demonstrated that substitutions of Cys at positions His19 and Trp23 result in reduced ion channel activity (28). However, the role of the cytoplasmic domain of the BM2 protein in ion channel activity has not been determined. In the case of influenza A virus, M2 molecules with truncated cytoplasmic domains display significantly reduced ion channel activity, indicating that the cytoplasmic domain is involved in the function of ion channel activity (45). If this is also the case for BM2, truncation of the cytoplasmic domain may affect ion channel activity. Thus, reduced ion channel activity of BM2 may represent one of the reasons for decreased virus infectivity. Using reverse-genetics techniques, we have observed that influenza B virus with amino acid changes at positions 19 and 23, causing defective ion channel activity, grows more slowly than wild-type virus in the multiple-step growth cycle but pro-

duces infectious progeny viruses with a maximum yield similar to that of wild-type virus (M. Obuchi, M. Imai, and T. Odagiri, unpublished observations). For the influenza A virus M2 protein, Watanabe et al. (48) suggested that ion channel activity is dispensable for growth in tissue culture, whereas Takeda et al. (43) argued against those findings following analysis of amantadine sensitivity and concluded that ion channel activity contributes to efficient virus replication. These studies suggest that H^+ ion channel activity is important for efficient growth of both influenza A and influenza B viruses but that activity may not be absolutely essential for virus viability in tissue culture.

We also found that truncation of the BM2 cytoplasmic domain significantly affects not only incorporation of vRNP into virions but also incorporation of M1. For influenza A virus M2, however, truncation of the cytoplasmic domain does not affect packaging of M1 into virions (16, 25). The reasons for this difference remain unclear, but we speculate that differences in the nature of protein-protein interactions for the vRNP-M1 complex between influenza A and influenza B viruses are re-
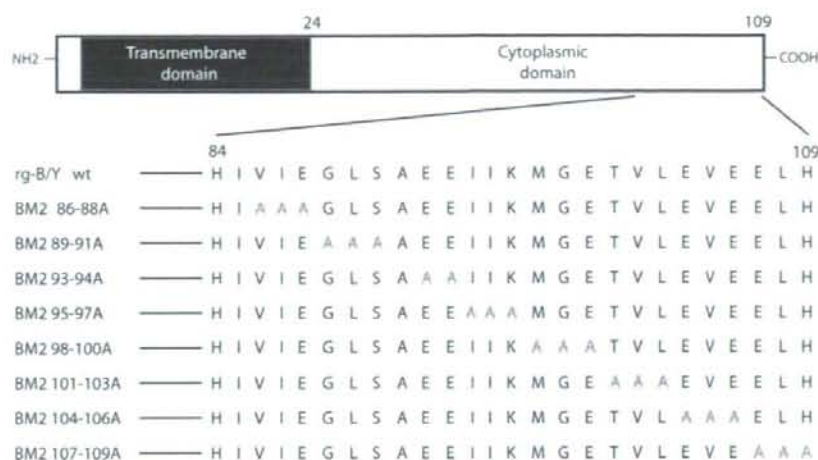
FIG. 8. Schematic diagram of wild-type and mutant BM2 proteins with alanine substitutions in the BM2 cytoplasmic domain. Amino acid sequence of the BM2 cytoplasmic domain (residues 84 to 109) is shown. Mutated amino acid residues are indicated in red for each BM2 mutant.

sponsible. Interestingly, complex formation among vRNP, M1, and NEP/NS2 of influenza B virus has been shown to differ from that with influenza A virus (15). Further characterization of interactions among viral components is required to elucidate the final steps of virus assembly.

The M1 protein is a multifunctional protein that plays central roles in virus assembly and budding. When expressed in cells, M1 can induce the formation and release of M1-containing particles into extracellular medium without the aid of other viral proteins (10, 19). The protein also exhibits lipid-binding properties (3, 11, 38) and associates tightly with cell membranes to form the inner surface of the lipid bilayer of the envelope (1, 6, 18, 51). Moreover, M1 interacts both with vRNP to mediate nuclear export and prevent nuclear reentry of vRNP (23, 50) and with cytoplasmic domains of the HA and NA proteins on the plasma membrane (1, 6, 17, 53). M1 thus appears to coordinate particle formation of influenza virus by forming a bridge between the lipid envelope and various virus components. We have previously shown that membrane association of influenza B virus M1 is highly influenced by the presence or absence of BM2 on the membrane (14). In the present study, we also observed that truncation of the BM2 cytoplasmic domain causes decreased membrane association of M1 by flotation gradient analysis, suggesting that the cytoplasmic domain of BM2 interacts with the M1 protein and increases the membrane-binding affinity of the M1 protein (Fig. 7). Support for this notion is provided by previous experiments in which BM2 was coprecipitated with M1 when detergent-disrupted virions were immunoprecipitated using anti-M1 antibody and by the finding that in experiments of virion fractionation, BM2 always coexists with M1 in the same fractions but is not present with HA and vRNP without M1 (32). Based on these findings, it is tempting to speculate that a major contribution of this M1-BM2 interaction is to capture M1-vRNP complex at the virion budding site during virus assembly. Interestingly, small amounts of M1 in BM2 mutant virions remained detectable when vRNP incorporation was drastically

reduced (Fig. 4 and 9). We therefore postulate that two populations of M1 molecules exist within virions: vRNP-associated M1 and vRNP-free M1. The cytoplasmic domain of the BM2 protein may selectively bind to vRNP-associated M1 but not to vRNP-free M1, since the number of BM2 molecules within infected cells is much lower than that of M1 molecules.

In addition to vRNP packaging, M1-BM2 interaction is likely to control the morphology of virus budding. Influenza B viruses with BM2 proteins containing altered cytoplasmic domains display a wide range of sizes and shapes relative to those of wild-type viruses, as determined by negative-staining electron microscopy (Fig. 5). Initially, M1 was thought to be the major driving force in virus budding (10, 19), although a subsequent study found that M1 of influenza A virus was not released efficiently into culture medium when M1 was expressed in the absence of other viral proteins, suggesting that M1 may not be required for virus budding (4). However, M1 is known to modulate virus particle morphology (2, 5). We therefore hypothesize that changes in the strength of M1-membrane interaction may down-regulate the efficiency of virus release, leading to significant changes in virus particle morphology. Our study using BM2 mutants suggested the importance of M1-BM2 interactions in the morphological features and assembly of influenza B virus. We also observed that BM2stop, BM2Δ104-109, and BM2Δ101-109 mutant particles with altered morphology had a much greater content of cellular actin than spherical virions, such as wild-type and BM2Δ107-109 viruses. The cellular cytoskeleton has been proposed to play an important role in bud formation and bud release of influenza virus. For influenza A virus, cellular actin and the actin-binding protein ezrin-radixinmoesin have been found in purified preparations of particles (39). Furthermore, disruption of the actin cytoskeleton inhibits the production of filamentous virions but not spherical virions, suggesting that formation depends on intact actin filaments (37, 42). Our data suggest that exclusion of a large proportion of actin from the viral budding site was impaired by deletion of the BM2 cytoplasmic domain. Efficient
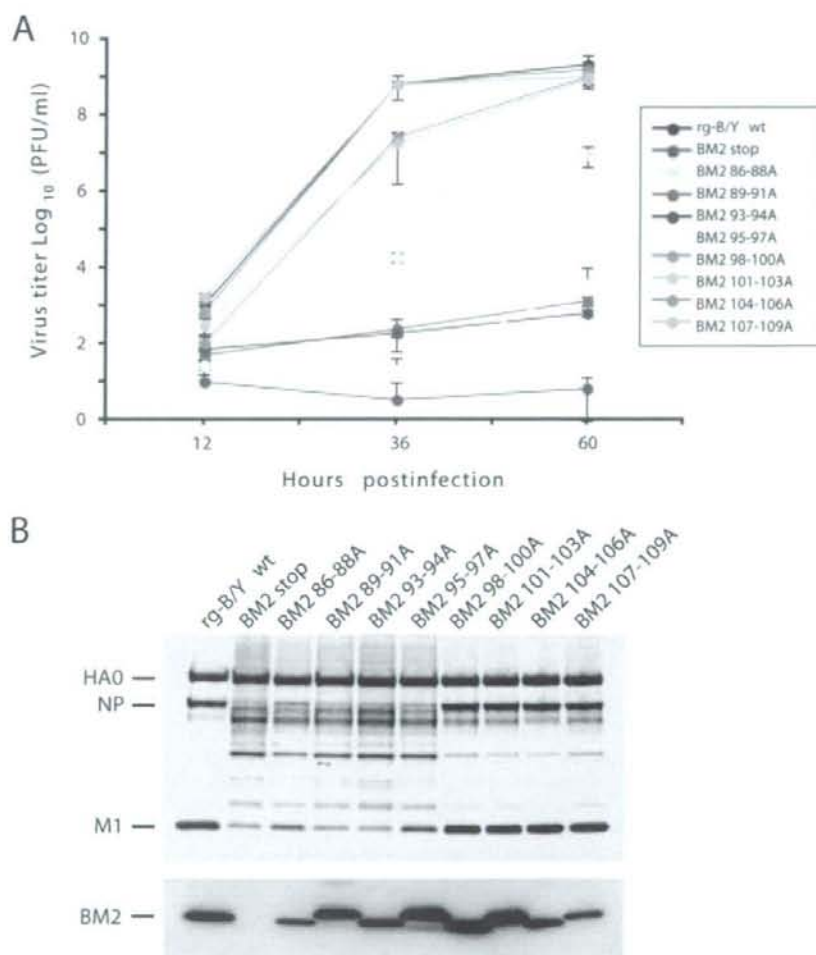
FIG. 9. Characterization of influenza B virus mutants with alanine substitutions in the cytoplasmic domain. (A) Multiple-step growth curve of BM2 mutant viruses. MDCK cells were infected at an MOI of 0.001 PFU, and culture medium was harvested at the indicated times. Virus yield of the supernatant was determined by plaque assay on CK/BM2 cells. (B) Protein composition of BM2 mutant virions. Proteins of purified viruses were analyzed by Coomassie brilliant blue staining (upper panel) and Western blotting using anti-BM2 antibody (lower panel).

exclusion of host proteins from virions might be involved in the maturation of spherical virus particles.

Previous studies have shown that sequences at both the 5′ and 3′ ends of the vRNA coding region are necessary for efficient incorporation of the vRNA segment into virions (8, 9, 20, 22, 29, 34, 49). We therefore cannot exclude the possibility that the mutations introduced into 5′ coding ends of the M segment disrupt packaging signals, resulting in reduced viral replication. However, we found that when the wild-type BM2 protein was supplemented by host cells expressing BM2, the BM2 cytoplasmic domain-truncated virus (BM2Δ104-109 mutant) exhibited growth kinetics indistinguishable from that of rg-B/Y wt virus, and no significant differences existed in the incorporation of the M1 protein between the mutant and wild-type viruses (Fig. 6). Consequently, we favor the interpretation

that viral infectivity was reduced as a result of truncation of the BM2 cytoplasmic domain.

Since truncation of the carboxyl-terminal three residues of BM2 (BM2Δ107-109) had no effect on production of infectious viruses but truncation of six or nine residues (BM2Δ104-109 or BM2Δ101-109) significantly impaired vRNP incorporation into particles, a six-amino-acid region encompassing residues 101 to 106 should contain an essential domain for production of infectious virus. However, we observed that neither alanine substitutions of residues 101 to 103 (BM2 101-103A) nor substitutions of residues 104 to 106 (BM2 104-106A) had any effect on infectious virus production. These observations suggest that the sequence in this region of the BM2 cytoplasmic domain is not critical for vRNP complex incorporation into virions but the actual length of the cytoplasmic domain might be important for fulfilling BM2 function.

Serial substitutions in the cytoplasmic domain of the BM2 protein indicated that a 12-amino-acid stretch between amino acids 86 and 97 cannot be replaced by other sequences to preserve the innate function of BM2 (Fig. 9). The region may contain effector signals for binding of the M1 protein, like the signal found with the M2 protein of influenza A virus (24). Another possibility is that this region has a secondary structure essential for the stability of the BM2 protein. Alternatively, since the BM2 protein has been shown to be modified by phosphorylation (32), a serine-to-alanine change at position 91 might result in the loss of a phosphorylation site, so the function of BM2 may be affected. However, phosphorylation of M2 in influenza A virus does not appear to be essential for virus replication (44). Further investigations in terms of these possibilities are needed.

In summary, the present study showed that the presence and maintenance of a long cytoplasmic domain in BM2 is important for the function of the BM2 protein in the membrane association of the M1 protein, incorporation of vRNP and M1 into virions, and particle morphology. Moreover, we have presented evidence that suggests the amino acid region from position 86 to position 97 in the BM2 cytoplasmic domain is a prerequisite for innate BM2 function. These findings greatly enhance our understanding of the molecular mechanisms underlying influenza virus assembly.

ACKNOWLEDGMENTS

REFERENCES

1. Ali, A., R. T. Avalos, E. Ponimaskin, and D. P. Nayak. 2000. Influenza virus assembly: effect of influenza virus glycoproteins on the membrane association of M1 protein. J. Virol. 74:8709–8719.
2. Bourmakina, S. V., and A. Garcia-Sastre. 2003. Reverse genetics studies on the filamentous morphology of influenza A virus. J. Gen. Virol. 84:517–527.
3. Bucher, D. J., I. G. Kharitonenkov, J. A. Zakomirdin, V. B. Grigoriev, S. M. Klimenko, and J. F. Davis. 1980. Incorporation of influenza virus M-protein into liposomes. J. Virol. 36:586–590.
4. Chen, B. J., G. P. Leser, E. Morita, and R. A. Lamb. 2007. Influenza virus hemagglutinin and neuraminidase, but not the matrix protein, are required for assembly and budding of plasmid-derived virus-like particles. J. Virol. 81:7111–7123.
5. Elleman, C. J., and W. S. Barclay. 2004. The M1 matrix protein controls the filamentous phenotype of influenza A virus. Virology 321:144–153.
6. Enami, M., and K. Enami. 1996. Influenza virus hemagglutinin and neuraminidase glycoproteins stimulate the membrane association of the matrix protein. J. Virol. 70:6653–6657.
7. Fouillot-Coriou, N., and L. Roux. 2000. Structure-function analysis of the Sendai virus F and HN cytoplasmic domain: different role for the two proteins in the production of virus particle. Virology 270:464–475.
8. Fujii, K., Y. Fujii, T. Noda, Y. Muramoto, T. Watanabe, A. Takada, H. Goto, T. Horimoto, and Y. Kawaoka. 2005. Importance of both the coding and the segment-specific noncoding regions of the influenza A virus NS segment for its efficient incorporation into virions. J. Virol. 79:3766–3774.
9. Fujii, Y., H. Goto, T. Watanabe, T. Yoshida, and Y. Kawaoka. 2003. Selective incorporation of influenza virus RNA segments into virions. Proc. Natl. Acad. Sci. USA 100:2002–2007.
10. Gomez-Puertas, P., C. Albo, E. Perez-Pastrana, A. Vivo, and A. Portela. 2000. Influenza virus matrix protein is the major driving force in virus budding. J. Virol. 74:11538–11547.
11. Gregoriades, A., and B. Frangione. 1981. Insertion of influenza M protein into the viral lipid bilayer and localization of site of insertion. J. Virol. 40:323–328.
12. Hatta, M., H. Goto, and Y. Kawaoka. 2004. Influenza B virus requires BM2 protein for replication. J. Virol. 78:5576–5583.
13. Helenius, A. 1992. Unpacking the incoming influenza virus. Cell 69:577–578.
14. Imai, M., S. Watanabe, A. Ninomiya, M. Obuchi, and T. Odagiri. 2004.

15. Influenza B virus BM2 protein is a crucial component for incorporation of viral ribonucleoprotein complex into virions during virus assembly. J. Virol. 78:11007–11015.
15. Imai, M., S. Watanabe, and T. Odagiri. 2003. Influenza B virus NS2, a nuclear export protein, directly associates with the viral ribonucleoprotein complex. Arch. Virol. 148:1873–1884.
16. Iwatsuki-Horimoto, K., T. Horimoto, T. Noda, M. Kiso, J. Maeda, S. Watanabe, Y. Muramoto, K. Fujii, and Y. Kawaoka. 2006. The cytoplasmic tail of the influenza A virus M2 protein plays a role in viral assembly. J. Virol. 80:5233–5240.
17. Jin, H., G. P. Leser, J. Zhang, and R. A. Lamb. 1997. Influenza virus hemagglutinin and neuraminidase cytoplasmic tails control particle shape. EMBO J. 16:1236–1247.
18. Kretzschmar, E., M. Bui, and J. K. Rose. 1996. Membrane association of influenza virus matrix protein does not require specific hydrophobic domains or the viral glycoproteins. Virology 220:37–45.
19. Latham, T., and J. M. Galarza. 2001. Formation of wild-type and chimeric influenza virus-like particles following simultaneous expression of only four structural proteins. J. Virol. 75:6154–6165.
20. Liang, Y., Y. Hong, and T. G. Parslow. 2005. cis-acting packaging signals in the influenza virus PB1, PB2, and PA genomic RNA segments. J. Virol. 79:10348–10355.
21. Macdonald, J. L., and L. J. Pike. 2005. A simplified method for the preparation of detergent-free lipid rafts. J. Lipid Res. 46:1061–1067.
22. Marsh, G. A., R. Hatami, and P. Palese. 2007. Specific residues of the influenza A virus hemagglutinin viral RNA are important for efficient packaging into budding virions. J. Virol. 81:9727–9736.
23. Martin, K., and A. Helenius. 1991. Nuclear transport of influenza virus ribonucleoproteins: the viral matrix protein (M1) promotes export and inhibits import. Cell 67:117–130.
24. McCown, M. F., and A. Pekosz. 2006. Distinct domains of the influenza a virus M2 protein cytoplasmic tail mediate binding to the M1 protein and facilitate infectious virus production. J. Virol. 80:8178–8189.
25. McCown, M. F., and A. Pekosz. 2005. The influenza A virus M2 cytoplasmic tail is required for infectious virus production and efficient genome packaging. J. Virol. 79:3595–3605.
26. Mebatsion, T., M. Konig, and K. K. Conzelmann. 1996. Budding of rabies virus particles in the absence of the spike glycoprotein. Cell 84:941–951.
27. Mitnaul, L. J., M. R. Castrucci, K. G. Murti, and Y. Kawaoka. 1996. The cytoplasmic tail of influenza A virus neuraminidase (NA) affects NA incorporation into virions, virion morphology, and virulence in mice but is not essential for virus replication. J. Virol. 70:873–879.
28. Mould, J. A., R. G. Paterson, M. Takeda, Y. Ohigashi, P. Venkataraman, R. A. Lamb, and L. H. Pinto. 2003. Influenza B virus BM2 protein has ion channel activity that conducts protons across membranes. Dev. Cell 5:175–184.
29. Muramoto, Y., A. Takada, K. Fujii, T. Noda, K. Iwatsuki-Horimoto, S. Watanabe, T. Horimoto, H. Kida, and Y. Kawaoka. 2006. Hierarchy among viral RNA (vRNA) segments in their role in vRNA incorporation into influenza A virions. J. Virol. 80:2318–2325.
30. Nayak, D. P., E. K. Hui, and S. Barman. 2004. Assembly and budding of influenza virus. Virus Res. 106:147–165.
31. Niwa, H., K. Yamamura, and J. Miyazaki. 1991. Efficient selection for high-expression transfectants with a novel eukaryotic vector. Gene 108:193–199.
32. Odagiri, T., J. Hong, and Y. Ohara. 1999. The BM2 protein of influenza B virus is synthesized in the late phase of infection and incorporated into virions as a subviral component. J. Gen. Virol. 80:2573–2581.
33. Oomens, A. G., K. P. Bevis, and G. W. Wertz. 2006. The cytoplasmic tail of the human respiratory syncytial virus F protein plays critical roles in cellular localization of the F protein and infectious progeny production. J. Virol. 80:10465–10477.
34. Ozawa, M., K. Fujii, Y. Muramoto, S. Yamada, S. Yamayoshi, A. Takada, H. Goto, T. Horimoto, and Y. Kawaoka. 2007. Contributions of two nuclear localization signals of influenza A virus nucleoprotein to viral replication. J. Virol. 81:30–41.
35. Paterson, R. G., M. Takeda, Y. Ohigashi, L. H. Pinto, and R. A. Lamb. 2003. Influenza B virus BM2 protein is an oligomeric integral membrane protein expressed at the cell surface. Virology 306:7–17.
36. Pinto, L. H., and R. A. Lamb. 2006. Influenza virus proton channels. Photochem. Photobiol. Sci. 5:629–632.
37. Roberts, P. C., and R. W. Compans. 1998. Host cell dependence of viral morphology. Proc. Natl. Acad. Sci. USA 95:5746–5751.
38. Ruigrok, R. W., A. Barge, P. Durrer, J. Brunner, K. Ma, and G. R. Whittaker. 2000. Membrane interaction of influenza virus M1 protein. Virology 267:289–298.
39. Sagara, J., S. Tsukita, S. Yonemura, S. Tsukita, and A. Kawai. 1995. Cellular actin-binding ezrin-radixin-moesin (ERM) family proteins are incorporated into the rabies virion and closely associated with viral envelope proteins in the cell. Virology 206:485–494.
40. Schmitt, A. P., B. He, and R. A. Lamb. 1999. Involvement of the cytoplasmic

domain of the hemagglutinin-neuraminidase protein in assembly of the paramyxovirus simian virus 5. J. Virol. 73:8703–8712.

41. Schmitt, A. P., G. P. Leser, D. L. Waning, and R. A. Lamb. 2002. Requirements for budding of paramyxovirus simian virus 5 virus-like particles. J. Virol. 76:3952–3964.

42. Simpson-Holley, M., D. Ellis, D. Fisher, D. Elton, J. McCauley, and P. Digard. 2002. A functional link between the actin cytoskeleton and lipid rafts during budding of filamentous influenza virions. Virology 301:212–225.

43. Takeda, M., A. Pekosz, K. Shuck, L. H. Pinto, and R. A. Lamb. 2002. Influenza a virus M2 ion channel activity is essential for efficient replication in tissue culture. J. Virol. 76:1391–1399.

44. Thomas, J. M., M. P. Stevens, N. Percy, and W. S. Barclay. 1998. Phosphorylation of the M2 protein of influenza A virus is not essential for virus viability. Virology 252:54–64.

45. Tobler, K., M. L. Kelly, L. H. Pinto, and R. A. Lamb. 1999. Effect of cytoplasmic tail truncations on the activity of the M(2) ion channel of influenza A virus. J. Virol. 73:9695–9701.

46. Waning, D. L., A. P. Schmitt, G. P. Leser, and R. A. Lamb. 2002. Roles for the cytoplasmic tails of the fusion and hemagglutinin-neuraminidase proteins in budding of the paramyxovirus simian virus 5. J. Virol. 76:9284–9297.

47. Watanabe, S., M. Imai, Y. Ohara, and T. Odagiri. 2003. Influenza B virus BM2 protein is transported through the trans-Golgi network as an integral membrane protein. J. Virol. 77:10630–10637.

48. Watanabe, T., S. Watanabe, H. Ito, H. Kida, and Y. Kawaoka. 2001. Influenza A virus can undergo multiple cycles of replication without M2 ion channel activity. J. Virol. 75:5656–5662.

49. Watanabe, T., S. Watanabe, T. Noda, Y. Fujii, and Y. Kawaoka. 2003. Exploitation of nucleic acid packaging signals to generate a novel influenza virus-based vector stably expressing two foreign genes. J. Virol. 77:10575–10583.

50. Whittaker, G., M. Bui, and A. Helenius. 1996. Nuclear trafficking of influenza virus ribonucleoproteins in heterokaryons. J. Virol. 70:2743–2756.

51. Zhang, J., and R. A. Lamb. 1996. Characterization of the membrane association of the influenza virus matrix protein in living cells. Virology 225:255–266.

52. Zhang, J., G. P. Leser, A. Pekosz, and R. A. Lamb. 2000. The cytoplasmic tails of the influenza virus spike glycoproteins are required for normal genome packaging. Virology 269:325–334.

53. Zhang, J., A. Pekosz, and R. A. Lamb. 2000. Influenza virus assembly and lipid raft microdomains: a role for the cytoplasmic tails of the spike glycoproteins. J. Virol. 74:4634–4644.

The Global Circulation of Seasonal Influenza A (H3N2) Viruses

Colin A. Russell,[1] Terry C. Jones,[1,2,3] Ian G. Barr,[4] Nancy J. Cox,[5] Rebecca J. Garten,[5] Vicky Gregory,[6] Ian D. Gust,[4] Alan W. Hampson,[4] Alan J. Hay,[6] Aeron C. Hurt,[4] Jan C. de Jong,[2] Anne Kelso,[4] Alexander I. Klimov,[5] Tsutomu Kageyama,[7] Naomi Komadina,[4] Alan S. Lapedes,[8] Yi P. Lin,[6] Ana Mosterin,[1,3] Masatsugu Obuchi,[7] Takato Odagiri,[7] Albert D. M. E. Osterhaus,[2] Guus F. Rimmelzwaan,[2] Michael W. Shaw,[5] Eugene Skepner,[1] Klaus Stohr,[9] Masato Tashiro,[7] Ron A. M. Fouchier,[2] Derek J. Smith[1,2*]

Antigenic and genetic analysis of the hemagglutinin of ~13,000 human influenza A (H3N2) viruses from six continents during 2002–2007 revealed that there was continuous circulation in east and Southeast Asia (E-SE Asia) via a region-wide network of temporally overlapping epidemics and that epidemics in the temperate regions were seeded from this network each year. Seed strains generally first reached Oceania, North America, and Europe, and later South America. This evidence suggests that once A (H3N2) viruses leave E-SE Asia, they are unlikely to contribute to long-term viral evolution. If the trends observed during this period are an accurate representation of overall patterns of spread, then the antigenic characteristics of A (H3N2) viruses outside E-SE Asia may be forecast each year based on surveillance within E-SE Asia, with consequent improvements to vaccine strain selection.

Influenza A (H3N2) virus is currently the major cause of human influenza morbidity and mortality worldwide. On average, influenza viruses infect 5 to 15% of the global population, resulting in ~500,000 deaths annually (1). Despite substantial progress in many areas of influenza research, questions such as when and to what extent the virus will change antigenically, and to what extent viruses spread globally, remain unanswered. A fundamental issue behind these questions is whether epidemics are the consequence of low-level persistence of viruses from the previous epidemic or whether they are seeded from epidemics in other regions and, if so, from where (2–8).

Addressing these issues of local persistence and global spread is vitally important for designing optimal surveillance and control strategies. If epidemics were regularly seeded from an outside region and if the source region of seed strains could be identified, it may be possible to forecast which variants would appear in epidemics in seeded regions and, consequently, to optimize vaccine strain selection. Alternatively, if viruses persist within a region, evolve, and reemerge to cause the next epidemic, intervention strategies targeting virus circulation between epidemics might be effective in minimizing subsequent epidemics.

The eight gene segments of influenza A viruses reassort, leading to complicated phylogenetic patterns at the genomic scale (4, 8–10). The gene segment coding for the hemagglutinin (HA) is of major importance because the HA protein is the primary target of the protective immune response. Consequently, the HA is the focus of public health surveillance and the primary component of currently licensed influenza vaccines. We used antigenic and genetic analyses of the HA as a marker to investigate the global evolution and epidemiology of influenza A (H3N2) viruses from 2002 to 2007 and to determine whether influenza epidemics arise from locally persisting strains or whether

epidemics are seeded from other regions.

Antigenic Evolution

Antigenic cartography has shown that the antigenic evolution of A (H3N2) virus, since its appearance in humans in 1968, can be represented by a two-dimensional (2D) antigenic map (11). Since 2002, the antigenic evolution of A (H3N2) viruses has roughly followed a line away from the A/Sydney/5/1997-like viruses that predominated in 1998 through the A/Fujian/441/2002-like viruses to the A/California/7/2004-like viruses to the A/Wisconsin/67/2005-like strains that predominated in 2006 and 2007. Figure 1A uses this directional bias to make a 2D plot to show spatial antigenic evolution and epidemiology in one plot.

Previously, Smith et al. (11) showed that, from 1968 to 2003, the antigenic evolution of A (H3N2) virus was punctuated: Periods of relative stasis lasting from 3 to 8 years were followed by rapid antigenic change, resulting in transitions to new antigenic clusters that necessitated an update of the influenza virus vaccine strain. During this time, several clusters also exhibited intracluster antigenic evolution, necessitating a within-cluster update of the vaccine strain. We find a similar pattern of intracluster antigenic evolution from 2002 to 2007. During this time, antigenic evo-

lution progressed away from A/Sydney/5/1997 at an average rate of 2.13 antigenic units per year (Fig. 1A). A distance of two antigenic units, representing a fourfold difference in hemagglutination inhibition (HI) assay titer, is generally considered as a sufficient antigenic difference to warrant a vaccine update. The A (H3N2) component of the influenza vaccine was updated four times during this period. A core component of vaccine strain selection involves identifying emerging antigenic variants. If an emerging variant is judged likely to cause epidemics in the upcoming influenza season, the vaccine is updated to contain a representative of the new strain.

We find differences in the amount of antigenic variation seen during an epidemic in different regions and from year to year in the same region (Fig. 1A). Despite such spatial and temporal heterogeneities, the antigenic evolution has been markedly homogeneous on a global scale. An explanation for this homogeneity could be that viruses circulate globally rather than persist and evolve locally.

To search for global patterns in the source of emerging variants, we measured which regions were leading or trailing antigenically and found that, from 2002 to 2007, newly emerged strains of the A (H3N2) subtype appeared in E-SE Asian countries, on average, ~6 to 9 months earlier than they appeared in other regions, with long delays to South America, typically of an additional ~6 to 9 months (Fig. 2A). Though A (H3N2) viruses in E-SE Asian countries are on average more antigenically advanced, there is sufficient variability from season to season (colored circles in Fig. 2A) such that no one particular country in the region is consistently most advanced. Thailand, Malaysia, and Japan are exceptions to the Asia-leading pattern, being less antigenically advanced than the rest of the region.

One interpretation of this Asia-leading pattern is that new variants emerge first in E-SE Asia and subsequently seed other regions of the world. An alternative but more complex explanation is that this pattern is the product of independent local persistence in multiple regions and parallel evolution in which similar antigenic variants emerge independently worldwide as a result of similar selection pressures. To test between these two interpretations, we must answer the fundamental long-standing question of whether influenza viruses persist in a region, and could thus undergo parallel evolution, or whether regions are regularly seeded from external regions.

About 10% of the ~13,000 A (H3N2) viruses analyzed antigenically were also analyzed genetically by sequencing the HA1 domain of the hemagglutinin (12). This subset was a representative sample of all ~13,000 isolates (fig. S1B) and thus was suitable for investigating the ancestry of strains and the fundamental issue of local persistence versus seeding in the global circulation of A (H3N2) viruses. The genetic progression over time (Fig. 1B) shows similar average patterns to the antigenic data, with Asia leading [as previously shown for Taiwan (13)] and South America trailing (Fig. 2,

[1]Department of Zoology, University of Cambridge, Cambridge, UK. [2]Department of Virology, Erasmus Medical Centre, Rotterdam, Netherlands. [3]Universitat Pompeu Fabra, Barcelona, Spain. [4]World Health Organization (WHO) Collaborating Centre for Reference and Research on Influenza, Melbourne, Australia. [5]WHO Collaborating Center for Influenza, Centers for Disease Control and Prevention, Atlanta, GA, USA. [6]WHO Collaborating Centre for Influenza, National Institute for Medical Research (NIMR), London, UK. [7]WHO Collaborating Center for Influenza, National Institute for Infectious Diseases, Tokyo, Japan. [8]Theoretical Division, Los Alamos National Laboratory, Los Alamos, NM, USA. [9]Novartis Vaccines and Diagnostics, Cambridge, MA, USA.

*To whom correspondence should be addressed. E-mail: dsmith@zoo.cam.ac.uk
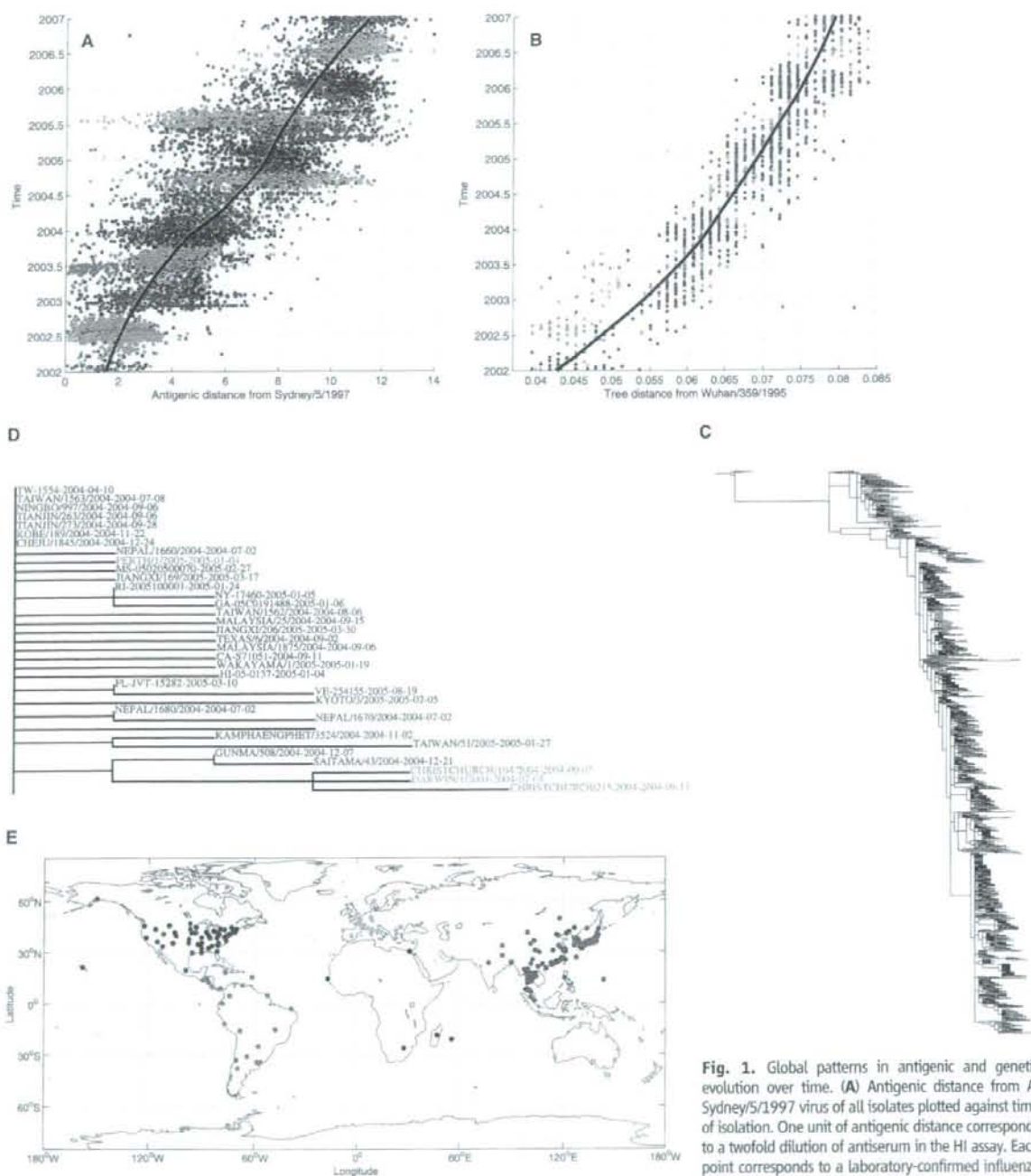
Fig. 1. Global patterns in antigenic and genetic evolution over time. (**A**) Antigenic distance from A/Sydney/5/1997 virus of all isolates plotted against time of isolation. One unit of antigenic distance corresponds to a twofold dilution of antiserum in the HI assay. Each point corresponds to a laboratory-confirmed influenza A (H3N2) isolate, with the color of the point indicating the region of geographic origin as shown in (E). The thick black line is the best-fit statistical model (a loess spline) fitted through all data points to show the trend over time. Points in advance of the spline are antigenically advanced, whereas strains behind the spline are antigenically lagging. (**B**) Genetic version of (A) for all sequenced strains with distance measured to the root, A/Wuhan/359/1995, of a maximum likelihood nucleotide phylogenetic tree (C). The thick black line is the same as in (A) but for the genetic data. (**C**) Phylogenetic tree of HA1 nucleotide sequences color-coded by geographic origin (E), including strain names and isolation dates. We constructed the initial tree with the PhyML software package version 2.4.5 (*38*), with 1567 nucleotide sequences (*12*) and A/Wuhan/359/1995 as the root, using GTR+I+Γ$_4$ (the general time-reversible model with the proportion of invariant sites and the gamma distribution of among-site rate variation with four rate categories estimated from the empirical data) [determined by ModelTest (*39*)] as the evolutionary model. GARLI version 0.951 (*40*) was run on the best tree from PhyML for two million generations to optimize tree topology and branch lengths. Figure S3A provides a "zoom-able" version of this image. (**D**) Partial detail of (C). (**E**) Color-coded geographic setting for (A) to (D).

A and B). However, there were important differences (China in 2005 and Oceania in 2005). For influenza vaccine strain selection, genetic-antigenic differences are resolved in favor of the antigenic data, because the humoral immune system "sees" the virus phenotype, not the genotype.

Persistence Versus Seeding

Source of inter-epidemic strains. The simplest test of persistence versus seeding is to examine the origin of strains isolated between epidemics. If viruses persist locally, at least some of the inter-epidemic strains would be descended from, and thus more closely related to, strains from the previous epidemic than to strains from outside the region. Alternatively, if there was no persistence, inter-epidemic strains would be more similar to strains from elsewhere.

We sequenced the HA1 domains of 52 inter-epidemic strains isolated in Oceania (primarily Australia and New Zealand), North America, and Japan from June 2002 to September 2006. None of these inter-epidemic strains was more similar to strains from the previous local epidemic than to externally circulating strains (Fig. 3). This result is evidence for external seeding and against local persistence.

Even when done well, inter-epidemic surveillance yields relatively small amounts of data that can never completely rule out the existence of local virus persistence between epidemics, especially of any low-pathogenic variants that produce subclinical infections. The test described in the next section has the advantage of using all available sequence data rather than being limited to inter-epidemic data. Nevertheless, all tests must take into account the effects of external introductions during local epidemics (14).

Evolutionary relationship of strains from one epidemic to the next in a region. As described by Nelson *et al.* (4, 8), if epidemic strains persist locally and give rise to the next local epidemic, those strains should be more closely related to one another than to strains isolated in other regions, and a phylogenetic tree of the data would look like that depicted in fig. S2A. Conversely, if epidemics were seeded from outside a region, the epidemic strains would be more similar to contemporary strains from outside that region than to strains from the previous local epidemic (fig. S2B).

Following the methodology of Nelson *et al.* (4, 8), we constructed a phylogenetic tree of the HA1 domain of the hemagglutinin from the sequenced subset of the global surveillance data (Fig. 1C and fig. S3A). In this tree, the HA1 of the viruses in each epidemic in a temperate region (four in North America, five in Oceania, four in Europe, and four in Japan) and each epidemic in a subtropical region (three in Hong Kong) descended from externally circulating strains, not from strains in the previous local epidemic (Fig. 1, C and D). The topology of this tree is more similar to that in fig. S2B than to that in fig. S2A. This result is also evidence for external seeding and against persistence. For other regions, including most tropical

and subtropical regions, there were fewer sequences, and it was not possible to conclusively differentiate between persistence and seeding.

This evidence for external seeding and against persistence agrees with full-genome analyses of New York state, Australia, and New Zealand data that show global migration of A (H3N2) viruses rather than local persistence (4, 8–10, 15). In addition, Nelson *et al.* (8) find evidence compatible with either northern-to-southern hemisphere migration or migration from tropical regions, including Southeast Asia.

Source of Seeding

Given this evidence for seeding and against local persistence, we are left with the interpretation that the E-SE Asia–leading pattern (Fig. 2, A and B) implies that new variants emerge first in E-SE Asia and then seed the rest of the world. The phylogenetic tree provides further evidence to support this interpretation, showing that the ancestors of strains in temperate regions typically originate in E-SE Asia, with the "trunk" of the phylogenetic tree typically occupied by E-SE Asian strains (Fig. 1, C and D) and with, on average, E-SE Asian strains closer to the trunk ($P < 0.001$) than strains from all other regions (Fig. 2C).

The above analyses, in addition to being evidence for an "out of E-SE Asia" hypothesis, are also evidence against several other long-standing unresolved hypotheses for the global circulation of influenza viruses, as follows.

Out-of-China. If China alone were the source of all new variants and effectively seeded the rest
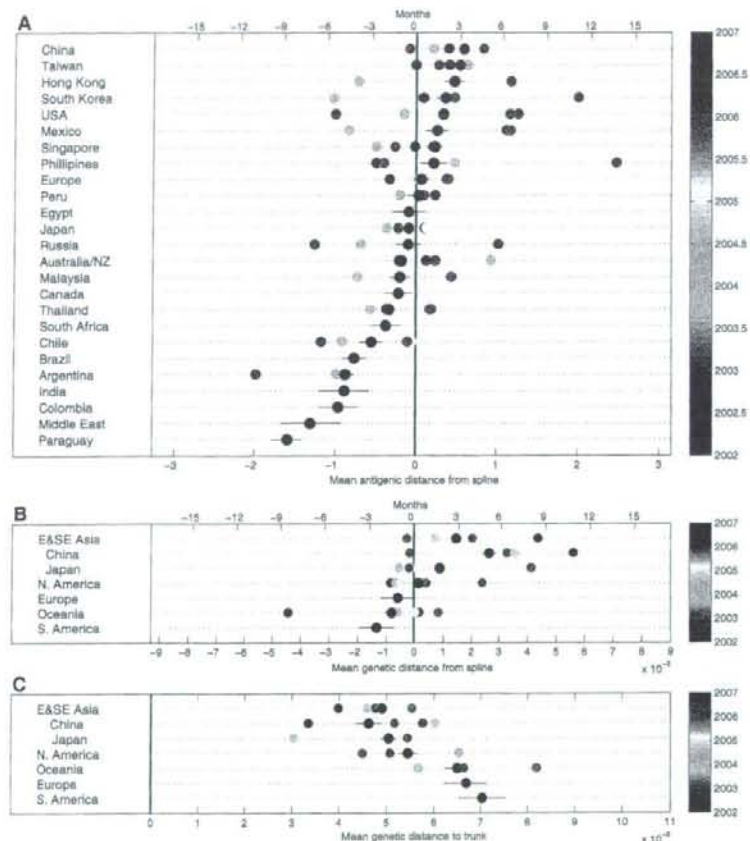
Fig. 2. Evolutionarily leading and trailing regions. (**A**) Black circles indicate the average antigenic distance to the spline of Fig. 1A for all strains isolated in a region, and the thin horizontal black line indicates the SEM. Colored circles split this overall average by epidemic; circle color indicates time. The spline can also be interpreted as a function of time; thus, time is shown as a second *x* axis. (**B**) Similar to (A) but based on genetic distance to spline from Fig. 1B. (**C**) Genetic distance to trunk of the phylogenetic tree by region and season. We algorithmically defined the trunk of the tree in Fig. 1C (14) and calculated the tree distance of each strain to the trunk. Average distance to trunk was calculated per region and per season. The black circles indicate the overall average per region, the thin horizontal black line indicates the SEM, and colored circles indicate seasonal averages. The mean for E-SE Asia is different from that of Oceania ($P < 0.00001$), North America ($P < 0.001$), Europe ($P < 0.01$), and South America ($P < 0.0001$).

of the world (16), then Chinese strains would be (i) closer to the trunk than strains from all other regions each year and (ii) consistently antigenically and genetically advanced relative to strains from other regions, both of which we do not find

(Fig. 2). Commensurate with previously published studies, we find new variants are sometimes first detected in China (15, 17, 18); however, we also find that new variants are sometimes first detected in other countries in E-SE Asia (Fig. 2).

Out-of-tropics. In this hypothesis, epidemics in regions outside the tropics are seeded from the tropics (7, 19). If true, A (H3N2) viruses would need to circulate continually in the tropics and would give rise to o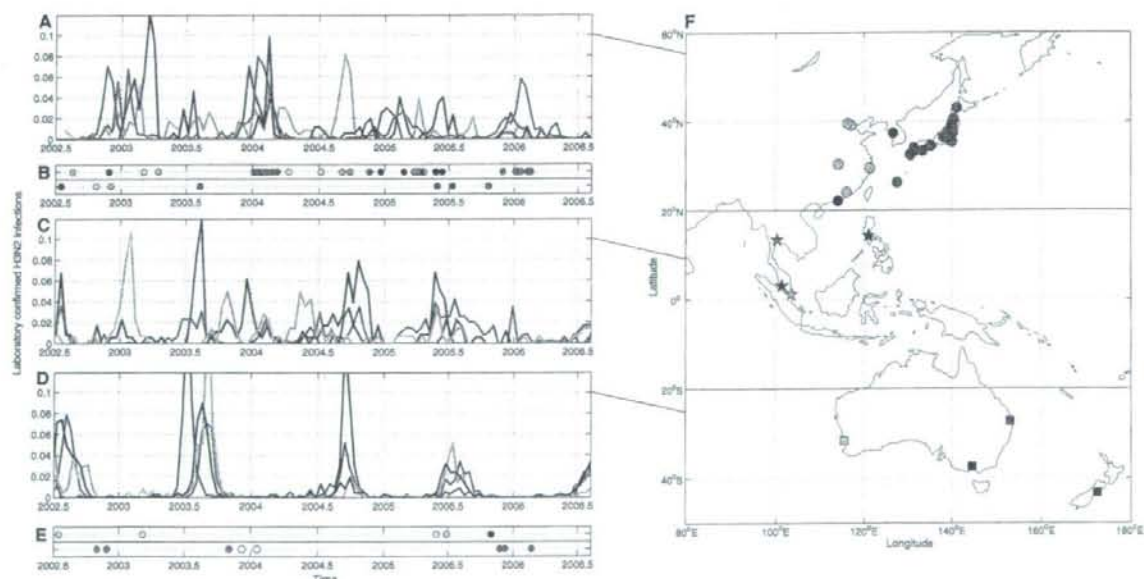ne of two evolutionary patterns. One pattern would arise if tropical Asia, Africa, and South America were well connected epidemiologically to one another; in this case, all three regions would be similarly antigenically and genetically advanced and closer to the trunk than nontropical regions. The other pattern would arise if the three tropical regions were poorly connected epidemiologically to one another; in this case, there would be independent genetic lineages for each tropical region. There is currently not enough data to include tropical Africa in this analysis. However, for tropical Asia and South America, neither of these patterns is observed (Figs. 1C and 2 and fig. S3A) (14).

Seeding by strains moving between the northern and southern hemispheres. If this hypothesis were true, then each year epidemics in the northern hemisphere would be seeded by viruses from epidemics in the southern hemisphere and vice versa (20–22). The phylogenetic tree for the HA1 domain (Fig. 1C and fig. S3A) shows no evidence for epidemic strains in the northern hemisphere being descendant from strains epidemic in South America or Africa. The tree shows limited evidence for Oceania playing a role in seeding a

Fig. 3. The genetic relationship of interseasonal strains to strains in the previous local epidemic and to strains epidemic in other regions. Interseasonal strains are defined as strains isolated more than 1 month after the end of the previous local epidemic and more than 1 month before the beginning of the next local epidemic. For each interseasonal strain, the phylogenetic tree distance was calculated to the closest strain in the previous epidemic and to the closest strain found outside the region in the previous 4 months. The diagonal line is 1:1 and is included for reference.

Fig. 4. Synchrony of epidemics in east Asia and the South Pacific. (**A**) Epidemics in east Asia. The y axis shows laboratory-confirmed H3N2 infections per 2 weeks as a proportion of the total number of laboratory-confirmed H3N2 infections over the study period in each location. (**B**) Strains on the trunk of the phylogenetic tree are of particular evolutionary importance in testing for virus migration among countries. In (B) and (E), there is a circle for every strain on the trunk of the phylogenetic tree (figs. S3A and S4). The purpose is to show where the trunk strains were isolated [top row color code from (A), bottom row from (C)] and when they were isolated, to assess the epidemiological activity at the time of isolation. Cyan circles represent E-SE Asian strains but in locations not shown in (F). (**C**) Same as (A) but for tropical Southeast Asia. (**D**) Same as (A) but for Australia and New Zealand. (**E**) Same as (B), but the top row are Oceanian strains [cyan circles represent strains from cities in Australia not shown in (F)], and the bottom row are strains from North America (blue) and Russia and Ukraine (yellow). (**F**) Geographic setting for (A) to (E).

minority of epidemics in the northern hemisphere (*14*) but at a level insufficient to support this hypothesis as the dominant mechanism of the global circulation of influenza viruses. This hypothesis also fails to explain how viruses from Asia, which is almost entirely contained within the northern hemisphere, lead antigenically and genetically and are closest to the trunk of the phylogenetic tree.

Local persistence with seeding only at cluster transitions. Though there was no major cluster transition during our study period, there has been an average of 2.13 units of antigenic evolution each year. Even so, in temperate regions, no local persistence could be detected, and each epidemic was seeded by exogenous strains. The drift variants observed in this study have emerged from E-SE Asia; however, because we have not seen a major cluster transition of the magnitude of Wuhan 1995 to Sydney 1997 (~4.7 antigenic units), we can neither exclude that in such a case a new variant could emerge outside E-SE Asia nor that it could affect seeding patterns.

The E-SE Asian Circulation Network

For E-SE Asia to seed epidemics in multiple regions of the world, influenza virus must circulate continually in E-SE Asia. But how?

It is generally considered that influenza viruses continually circulate in tropical countries (*7*, *23–27*) and, if this were true, it would explain how influenza viruses could persist in tropical Asia. Indeed, circulation in an endemic core area that seeds satellite areas has been shown to be a key epidemiological process for the continual circulation of antigenically stable pathogens (*28*, *29*). Reports based on influenza-like illness (ILI) or influenza and pneumonia mortality (IPM) data describe continual circulation in the tropics (*23*). However, several viruses other than influenza can cause ILI and IPM, and studies from tropical countries based on viral isolations show a marked seasonality for influenza epidemics, with peaks usually occurring during periods of high rainfall (*30–35*). In agreement with these studies based on virus isolation, our virus isolation study also finds that influenza has clear epidemic peaks and deep troughs in all regions, including the four

tropical and four subtropical E-SE Asian countries for which there are sufficient data to detect an epidemic signal. Thus, continuous circulation in individual tropical countries is unlikely to be the mechanism for persistence in E-SE Asia. However, more data from a wide diversity of locations are needed to fully understand seasonal forcing and to definitively exclude local persistence as an element of transmission dynamics in tropical and subtropical areas of E-SE Asia.

Another possibility for continual circulation is that viruses pass from epidemic to epidemic among countries via the mobile human population. Figure 4, A and C, shows that there is sufficient variability in the timing of epidemics within E-SE Asia such that the virus could circulate continuously in this way as a result of the temporal overlap of epidemics. Much of the variability in the timing of epidemics is likely to be linked to the heterogeneity in the timing of lower temperatures and rainy seasons (*19*, *33*, *36*). We thus hypothesize that the variability of epidemics, combined with the interconnectedness of E-SE Asian countries, forms an E-SE Asian circulation network that maintains influenza virus in the region by passing from epidemic to epidemic.

If such a network existed, we would expect a temporal and phylogenetic progression of E-SE Asian viruses on the trunk of phylogenetic tree as viruses pass from epidemic to epidemic within the network. Figure S4 shows such a progression, and Fig. 4, B and E, shows the relationship of these trunk strains to the timing of epidemics. Trunk strains were isolated in temperate, subtropical, and tropical regions of E-SE Asia, indicating that all three climatic regions of E-SE Asia are part of the circulation network. To test whether the non–E-SE Asian strains on the trunk indicate that the circulation network includes countries outside of E-SE Asia or whether they represent one-way seeding events out of E-SE Asia, we examined the phylogenetic tree (Fig. 1C and fig. S3A). We found only limited instances of such seeding back into E-SE Asia, with clear evidence that most E-SE Asian strains were directly descendent from other E-SE Asian strains (*14*)—thus indicating that the temporally overlapping epidemics in E-SE Asia form a circulation network that, during the

study period, has been mostly closed to external reseeding.

E-SE Asia's strong travel and trade connections to Oceania, North America, and Europe (*14*, *37*) facilitate the rapid movement of new influenza virus variants into those areas and thus explain the relatively small lag in antigenic and genetic advancement seen in those regions (Fig. 2, A and B). Also, though it is unclear how much travel there must be between two locations for them to be epidemiologically well-connected, South America's 6- to 9-month antigenic lag (Fig. 2A) may be attributable to its paucity of direct connections with E-SE Asia (fig. S5). South America's strong travel connections to Europe and North America, but not to E-SE Asia, could result in a seeding hierarchy where strains are first seeded into North America and Europe and from there to South America (Fig. 5). Most strains appear to circulate in this simple hierarchy, and even those strains that circulate in a more complex hierarchy still originate in E-SE Asia (*14*). Thus, the extinction of many H3 lineages—a key characteristic of the H3 phylogeny—may, in addition to the accumulation of deleterious mutations (*25*), also be due to reaching the end of this hierarchy.

Surveillance and Vaccine Strain Selection

A major practical function of WHO's Global Influenza Surveillance Network is to assist regulatory authorities to recommend which strains should be included in influenza vaccines. Expanding surveillance within the E-SE Asian circulation network will aid the early detection of the emergence and spread of new variants and could help to more precisely define the network. Such surveillance is crucial for optimizing vaccine strain selection for countries within the network and for forecasting which variants will seed epidemics in the rest of the world, consequently increasing vaccine efficacy and ultimately reducing influenza morbidity and mortality worldwide.

Given the importance of the HA, it is the only portion of the virus genome that is currently sequenced routinely within the WHO Global Influenza Surveillance Network. Recently, whole-genome sequencing initiatives have provided important insights into the genesis and spread of reassortment viruses, their rapid migration, and the cocirculation of multiple lineages (*4*, *8*, *9*, *15*). Expanded sequencing of whole genomes will provide additional markers for tracking the global migration of viruses and reveal potential differences between the global evolution of the HA and the other gene segments. Such sequencing efforts should include strains from E-SE Asia and be linked with antigenic data on HA and, in the longer term, with phenotype changes determined by other virus genes to fully understand the selection pressures on influenza viruses and their epidemiology.

The data used in this study were generated by the WHO Global Influenza Surveillance Network. Although there are biases in surveillance data, these biases do not have a substantial effect on the results (*14*). The methods we have used are
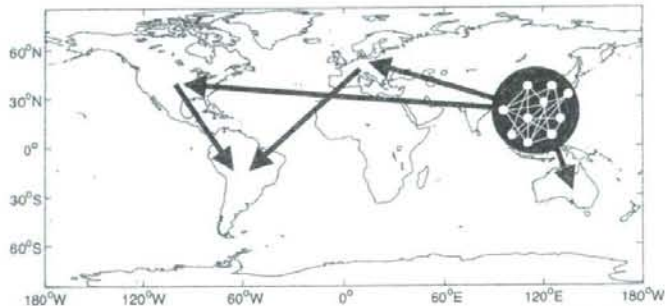

Fig. 5. Schematic of the dominant seeding hierarchy of seasonal influenza A (H3N2) viruses. The structure of the network within E-SE Asia is unknown.

generic and, although applied here to human influenza A (H3N2) viruses, are broadly applicable to influenza viruses in other species and to other pathogens.

Summary

We present evidence from antigenic and genetic analyses of HA that, from 2002 to 2007, influenza A (H3N2) virus epidemics worldwide were seeded each year by viruses that originated in E-SE Asia. We find evidence that temporally overlapping epidemics in E-SE Asia create a circulation network in which influenza A (H3N2) viruses continually circulate within the region by passing from epidemic to epidemic. E-SE Asia's strong travel and trade connections with Oceania, North America, and Europe, coupled with weak connections to South America, could explain the seeding hierarchy observed in this period where new virus variants first seed epidemics in Oceania, North America, and Europe and later in South America. The mostly one-way nature of this hierarchy suggests that, once A (H3N2) viruses leave E-SE Asia, they are unlikely to contribute to long-term viral evolution. If the trends observed during this period are an accurate representation of overall patterns of spread, then the antigenic characteristics of A (H3N2) viruses outside E-SE Asia may be forecast each year based on surveillance within E-SE Asia, with consequent improvements to vaccine strain selection and reductions in influenza A (H3N2) morbidity and mortality. Intensified surveillance, including whole-genome sequencing, and better understanding of the evolutionary selection pressures in E-SE Asia would further improve vaccine strain selection worldwide and potentially make influenza virus evolution more predictable.

References and Notes

1. K. Stohr, *Lancet Infect. Dis.* **2**, 517 (2002).
2. Commission on Acute Respiratory Diseases, *Am. J. Hyg.* **47**, 290 (1948).
3. J. A. Dudgeon, C. H. Stuart-Harris, C. H. Andrewes, R. E. Glover, W. H. Bradley, *Lancet* **248**, 627 (1946).
4. M. I. Nelson et al., *PLoS Pathog.* **2**, e125 (2006).
5. R. M. Taylor, *Am. J. Public Health* **39**, 171 (1949).
6. S. B. Thacker, *Epidemiol. Rev.* **8**, 129 (1986).
7. C. Viboud, W. J. Alonso, L. Simonsen, *PLoS Med.* **3**, e89 (2006).
8. M. I. Nelson, L. Simonsen, C. Viboud, M. A. Miller, E. C. Holmes, *PLoS Pathog.* **3**, e131 (2007).
9. E. C. Holmes et al., *PLoS Biol.* **3**, e300 (2005).
10. E. Ghedin et al., *Nature* **437**, 1162 (2005).
11. D. J. Smith et al., *Science* **305**, 371 (2004).
12. Sequences were deposited in the GenBank database (accession numbers EU501119 to EU502618 and EU514616 to EU514683). Table S1 contains the sequence name, accession number, and country of isolation for each strain.
13. S. R. Shih et al., *J. Clin. Microbiol.* **43**, 1651 (2005).
14. Materials and methods are available as supporting material on *Science* Online.
15. L. Simonsen et al., *Mol. Biol. Evol.* **24**, 1811 (2007).
16. K. F. Shortridge, *Chin. Med. J. (Engl.)* **110**, 637 (1997).
17. N. J. Cox, T. L. Brammer, H. L. Regnery, *Eur. J. Epidemiol.* **10**, 467 (1994).
18. N. J. Cox, K. Subbarao, *Annu. Rev. Med.* **51**, 407 (2000).
19. W. J. Alonso et al., *Am. J. Epidemiol.* **165**, 1434 (2007).
20. W. P. Glezen, R. B. Couch, in *Viral Infections of Humans*, A. S. Evans, Ed. (Plenum Medical Book Company, New York, 1989), pp. 419–449.
21. J. S. Nguyen-Van-Tam, in *Textbook of Influenza*, K. G. Nicholson, R. G. Webster, A. J. Hay, Eds. (Blackwell Science, London, 1998), pp. 181–206.
22. C. Viboud et al., *Emerg. Infect. Dis.* **10**, 32 (2004).
23. K. A. Fitzner, S. M. McGhee, A. J. Hedley, K. F. Shortridge, *Hong Kong Med. J.* **5**, 87 (1999).
24. A. S. Monto, *Int. Congr. Ser.* **1263**, 3 (2004).
25. M. I. Nelson, E. C. Holmes, *Nat. Rev. Genet.* **8**, 196 (2007).
26. J. M. Simmerman et al., *Vaccine* **23**, 182 (2004).
27. C. M. Wong et al., *PLoS Med.* **3**, e121 (2006).
28. B. T. Grenfell, O. N. Bjornstad, J. Kappey, *Nature* **414**, 716 (2001).
29. B. T. Grenfell, B. M. Bolker, *Ecol. Lett.* **1**, 63 (1998).
30. F. T. Chew, S. Doraisingham, A. E. Ling, G. Kumarasinghe, B. W. Lee, *Epidemiol. Infect.* **121**, 121 (1998).
31. T. S. David-West, A. R. Cooke, *Bull. WHO* **51**, 103 (1974).
32. E. de Arruda et al., *J. Infect. Dis.* **164**, 252 (1991).
33. S. Doraisingham, K. T. Goh, A. E. Ling, M. Yu, *Bull. WHO* **66**, 57 (1988).
34. A. Dosseh, K. Ndiaye, A. Spiegel, M. Sagna, C. Mathiot, *Am. J. Trop. Med. Hyg.* **62**, 639 (2000).
35. B. L. Rao, K. Banerjee, *Bull. WHO* **71**, 177 (1993).
36. L. P.-C. Shek, B.-W. Lee, *Paediatr. Respir. Rev.* **4**, 105 (2003).
37. L. Hufnagel, D. Brockmann, T. Geisel, *Proc. Natl. Acad. Sci. U.S.A.* **101**, 15124 (2004).
38. S. Guindon, O. Gascuel, *Syst. Biol.* **52**, 696 (2003).
39. D. Posada, K. A. Crandall, *Bioinformatics* **14**, 817 (1998).
40. D. J. Zwickl, thesis, University of Texas (2006).
41. We thank the many individuals throughout the WHO Global Influenza Surveillance Network, particularly those in National Influenza Centers, for their enormous contributions to surveillance; the maintainers of the Influenza Sequence Database (www.flu.lanl.gov), D. Burke, D. Horton, G. Lewis, N. Lewis, B. Mansell, D. M. Smith, K. Wuichet, and J.-C. Yeh; and the reviewers whose comments and suggestions substantially improved the manuscript. This work was supported by an NIH Director's Pioneer Award to D.J.S., part of the NIH roadmap for medical research, through grant number DP1-OD000490-01. R.A.M.F. is supported by National Institute of Allergy and Infectious Diseases–NIH contract HHSN266200700010C, as well as by the De Nederlandse Organisatie voor Wetenschappelijk Onderzoek Netherlands Influenza Vaccine Research Centre. The Melbourne WHO Collaborating Centre for Reference and Research on Influenza is supported by the Australian Government Department of Health and Aging. The WHO Collaborating Centre for Influenza, NIMR, UK, is funded by The Medical Research Council (UK). For the antigenic cartography software, see www.antigenic-cartography.org. The conclusions presented in this paper are those of the authors and do not necessarily reflect those of the funding agencies.

ELSEVIER

Timely production of A/Fujian-like influenza vaccine matching the 2003–2004 epidemic strain may have been possible using Madin–Darby canine kidney cells

Keiichi Makizumi[a,*], Kazuhiko Kimachi[a], Katsuhiko Fukada[a], Tomohiro Nishimura[a], Yasuhiro Kudo[a], Shuro Goto[a], Takato Odagiri[b], Masato Tashiro[b], Yoichiro Kino[a]

[a] The Chemo-Sero-Therapeutic Research Institute, Kyokushi, Kikuchi, Kumamoto 869-1298, Japan
[b] National Institute of Infectious Diseases, WHO Collaborating Center for Reference & Research on Influenza, Gakuen 4-7-1, Musashi-Murayama, Tokyo, 208-0011, Japan

ARTICLE INFO

ABSTRACT

Timely production and antigenic match with those of the epidemic strains are required for influenza vaccines. A/Fujian/411/2002-like (H3N2) virus was the main epidemic influenza virus during the 2003/2004 season in the northern hemisphere. But A/Fujian-like reassortant viruses were not available until more than one year later. We evaluated the A/Kumamoto/102/2002 strain, an A/Fujian/411/2002-like strain isolated in 2002, as a potential vaccine. We compared A/Kumamoto/102/2002 viruses isolated from the same clinical sample in Madin–Darby canine kidney (MDCK) cells and eggs. Kumamoto/102/2002 isolated from eggs grew poorly and showed amino acid mutations of haemagglutinin. In contrast, A/Kumamoto/102/2002 isolated from MDCK cells grew well in MDCK suspension culture. The amino acid sequence of MDCK-derived A/Kumamoto virus was identical to that of A/Fujian/411/2002. These results suggest that culture in MDCK cells could have produced an influenza vaccine with a better antigenic match to the predicted epidemic strain for the 2003/2004 season than the vaccine actually produced.

© 2008 Elsevier Ltd. All rights reserved.

1. Introduction

Influenza vaccines currently used around the world are manufactured from viral strains that are chosen to be antigenically similar to anticipated epidemic strains. The World Health Organization (WHO) makes a recommendation about the influenza virus strains that should be used for vaccine production for the northern hemisphere in February and for the southern hemisphere in September, based on analysis of the strains that are circulating predominantly at the time. Most influenza vaccines are manufactured by using embryonated chicken eggs as a substrate for viral growth. Therefore, only viral strains that show good replication in eggs can actually be used for vaccine production. For this reason and to avoid contamination with other human respiratory viruses, vaccine seed viruses should be isolates derived in eggs. However, some clinical isolates fail to grow or show poor replication in eggs. In such cases, to improve the growth of the desired viral strain, a reassortant virus is created by using the haemagglutinin (HA) and neuraminidase (NA) genes derived from the epidemic strain and other genes derived from the high yielding PR-8 strain [1].

However, it takes time to develop PR-8-based reassortant strains and it is sometimes impossible to establish a reassortant virus that is antigenically equivalent to the recommended strain. In recent years, the reverse genetics (RG) technique has made it easier to create reassortant strains suitable for vaccine production. However, viruses created by this technique are regarded as genetically modified organisms (GMO) in some countries. Therefore, the need for biological confinement of RG viruses during vaccine production means that this technique is not used to produce influenza vaccines at present.

In the spring of 2003, the WHO held its annual meeting to recommend influenza vaccine strains for the northern hemisphere 2003/2004 flu season. At that time, it was considered that an A/Fujian/411/2002-like (H3N2) strain might emerge as a result of antigenic drift from the A/Moscow-like strain that had been used in influenza vaccines during the previous year, but the WHO finally decided to recommend the A/Moscow-like strain vaccine again. One reason for choosing the A/Moscow-like strain over the A/Fujian-like strain was the lack of a viral strain that was antigenically equivalent to A/Fujian/411/2002 that showed good growth in eggs [2]. As a result, the vaccine manufacturers used the A/Panama/2007/99 strain (an A/Moscow/10/99-like virus) as the H3N2 component of vaccines for the 2003/2004 season. Subsequently, H3N2 strains were predominant during the flu season from

* Corresponding author. Tel.: +81 968 37 4090; fax: +81 968 37 3616.
E-mail address: makizumi@kaketsuken.or.jp (K. Makizumi).

Fig. 1. History of the A/Kumamoto/102/2002 viruses. A solid line arrow shows passage in MDCK-33016. A solid double line arrow shows cultivation in MDCK CCL34. A dotted line arrow shows passage in eggs. Viral growth was measured for 3 passages each of A/Ku M1, A/Ku E3, A/Ku E5, and A/Ku IVR-135 E12/E2. HA1 gene sequences were compared for A/Ku M1, A/Ku M1/M2, A/Ku E3, A/Ku E3/M2, A/Ku E5, A/Ku E5/M2, A/Ku IVR-135. E12/E2, and A/Ku IVR-135 E12/E2/M2. Viruses purified from A/Ku M1/M3, A/Ku E3/M3, A/Ku E5/M3, and A/Ku IVR-135 E12/E2/M3 were used for immunogenicity assays. To compare the HA content, A/Ku M1/M3, A/Ku E3/M3, A/Ku E5/M3, and A/Ku IVR-135 E12/E2/M3 were re-cultured from previously passaged viruses (/M2).

the winter of 2003 to the spring of 2004, and the A/Fujian-like strain was the most prominent of the H3N2 strains [3]. This resulted in a mismatch between the influenza vaccine and the predominant epidemic influenza virus [4].

In January 2002, the A/Kumamoto/102/2002 virus was isolated from a clinical specimen (swab) in southern Japan using Madin–Darby canine kidney (MDCK) cells (ATCC CCL-34) and it was found to have antigenic properties similar to that of A/Fujian/411/2002. This virus was re-isolated from the same clinical specimen using embryonated hens' eggs. Subsequently, a reassortant strain was generated from this egg-derived virus and was designated as A/Kumamoto/102/2002 IVR-135. This reassortant virus became one of the influenza vaccine candidates for the 2004/2005 season. Thus, it took 2 years to establish a reassortant vaccine seed candidate after isolation of the wild strain. Finally, A/Wyoming/3/2003 was recommended as the A/Fujian/411/2002-like strain for the 2004/2005 season.

We have been developing influenza vaccines by using suspension culture of the virus in MDCK cells. It has been reported that MDCK cells show lower selectivity for influenza virus than eggs, so that the generation of reassortant viruses may be unnecessary for the production of vaccines with these cells [5]. However, few authors have attempted to confirm this with viruses isolated from both MDCK cells and eggs that originated from the same clinical specimen. We recently obtained a paired set of A/Kumamoto/102/2002-related viruses, comprising the original isolates from MDCK cells and eggs, respectively, viruses passaged in these two substrates, and a high growth reassortant developed for egg culture. Using these viruses and suspension culture in MDCK cells, we investigated whether it was possible to obtain an influenza vaccine that showed a better antigenetic match with the predicted epidemic strain than the actual vaccine produced from embryonated eggs for the 2003/2004 influenza season.

2. Materials and methods

2.1. Viruses

We studied four A/Kumamoto/102/2002-related viruses (2002 0758 MDCK 1G 15.1.7, A/Kumamoto/102/2002 E3, A/Kumamoto/102/2002 E5, and A/Kumamoto/102/2002 IVR-135), as well as A/Wyoming/3/2003 IVR-134 and A/Wyoming/3/2003 X-147.

The history of the A/Kumamoto/102/2002 viruses is summarized in Fig. 1.

In January 2002, the A/Kumamoto/102/2002 virus was isolated from a clinical specimen at the Kumamoto Prefectural Institute of Public Health and Environmental Science (Kumamoto, Japan) using MDCK (ATCC CCL-34) cells. This virus was originally named '2002 0759 MDCK 1G 15.1.7' (A/Ku M1) and was sent to the National Institute of Infectious Diseases (NIID). In March 2003, The Chemo-Sero-Therapeutic Research Institute started to re-isolate this virus from the same specimen (swab) using embryonated hens' eggs. The isolated virus was passaged 3 times in eggs and then was sent to NIID as "A/Kumamoto/102/2002 E3 (A/Ku E3)" on March 17, 2003. Next, A/Ku E3 was passaged twice more in embryonated eggs at Kaketsuken and was harvested as "A/Kumamoto/102/2002 E5 (A/Ku E5)". Growth of both A/Ku E3 and A/Ku E5 in embryonated eggs was not adequate for vaccine production. Subsequently, A/Ku E3 was sent to CSL (Melbourne, Australia) and a high growth reassortant with PR-8 was generated. This reassortant strain was designated as A/Kumamoto/102/2002 IVR-135. We obtained this reassortant through the NIID at E12/E2 (A/Ku IVR-135 E12/E2), and A/Ku IVR-135 E12/E2 became one of the influenza vaccine candidates for 2004/2005 season.

A/Wyoming/3/2003 IVR-134 E13/E2 (A/Wy IVR-134 E13/E2) and X-147 E5/E2 (A/Wy X-147 E5E2) were actually used as A/Fujian-like vaccine strains in Japan and Europe for the 2004/2005 season. These

strains were also tested for growth in MDCK cells and embryonated eggs to allow comparison of viral growth and HA gene sequences in the following experiments.

2.2. Seed virus preparation

MDCK cells (MDCK-33016) developed by Novartis Vaccine and Diagnostic (Marburg, Germany) [6,7] were used throughout the study. The cells were cultured in 100-mL spinner flasks using serum-free medium. Each viral strain was passaged twice consecutively in the MDCK-33016 cells to establish seed viruses for pilot cell culture. Inoculated cells were grown in serum-free chemically defined medium containing 1 μg/mL trypsin at 34 °C for 3 days. Then the cells were removed by centrifugation, the supernatant was collected, and its infectivity titer was measured [8].

2.3. Pilot viral culture in MDCK cells and eggs

The cells cultured in 100-mL spinner flasks were inoculated with seed viruses at a multiplicity of infection (MOI) of 10^{-3}, 10^{-4}, or 10^{-5} (based on the titer of the seed virus). Then the inoculated cells were cultured in serum-free medium containing 1 μg/mL trypsin at 34 °C for 3 days, after which the cells were removed by centrifugation, the supernatant was collected, and its HA titer was measured. Virus was purified directly from the medium by ultracentrifugation on a 30% glucose cushion (112,700 × g for 150 min) to estimate the viral yield. After centrifugation, the viral pellet was collected and suspended in phosphate-buffered saline (PBS). Then the suspension was adjusted to the original volume of the culture supernatant and its HA content was measured by a single radial immunodiffusion (SRD) assay.

As a control, the four viruses (A/Ku M1, A/Ku E1, A/Ku E5 and A/Ku IVR-135 E12/E2) and A/Wy IVR-134 E13/E2 were also cultured in eggs. The viruses were inoculated into the chorioallantoic cavity of embryonated eggs at concentrations of 10^{-2} to 10^{-4} EID$_{50}$/0.2 mL. The inoculated eggs were incubated at 34 °C for 3 days and then were left overnight at 4 °C. Subsequently, the allantoic fluid was centrifuged at 320 × g for 10 min, 10 mL of supernatant was centrifuged at 102,300 × g for 60 min to pellet the virus, and the pellet was re-suspended in 100 μL of PBS. Then the HA content was measured by the SRD assay. We used the reagents for A/Wyoming in all SRD assays because we could not obtain any reagents for the A/Kumamoto virus.

2.4. HA1 gene sequencing

The HA1 gene sequences of the original viruses that we had obtained and the seed viruses that we established after passaging in MDCK cells and eggs were analyzed to investigate the occurrence of selection during culture in the cells or eggs.

The method employed was reported previously [9].

In brief, viral RNA was extracted with a Catrimox-14TM RNA Isolation Kit Ver. 2.11 (TaKaRa). RT-PCR was performed using the extracted viral RNA and primers to amplify HA genes with the TaKaRa One Step RNA PCR Kit (AMV) (TaKaRa). The primers were designed by using gene analysis software Genetix. The PCR products were separated by electrophoresis on 0.7% agarose gel and the part of the gel containing the HA gene region was cut out. Then DNA was harvested from the gel using Quantum Prep Freeze 'N Squeeze DNA (Bio-Rad), and was purified by phenol/chloroform treatment and ethanol precipitation. Finally, the gene sequence was analyzed using primers designed for sequencing and a Beckman CEQ2000XL capillary sequencer [10].

Table 1
Growth of A/Fujian-like viruses in MDCK-33016 cells.

Viruse	Passage[a]		
	1st (M1)	2nd (M2)	3rd (M3)
A/Ku M1	9.3[b]	8.9	8.6
A/Ku E3	7.9	8.9	8.9
A/Ku E5	8.1	8.6	8.1
A/Ku IVR135 E12/E2	7.3	8.6	9.0
A/Wy IVR-134 E13/E2	7.5	8.5	8.9
A/Wy X-147 E5/E2	6.8	7.9	9.3

[a] Viruses were passaged 3 times.
[b] Viral titers of culter supernatant were determined by the TCID assay. Titers are shown as log(TCID$_{50}$/ml).

2.5. Immunogenicity

The animal study was approved by our institutional Animal Experimentation Ethics Committee. The immunogenicity of the four A/Kumamoto viruses (A/Ku M1/M1 and A/Ku IVR-135 E12/E2/M3) was compared in Balb/c mice.

First, these viruses were purified and inactivated according to the following procedure. Culture supernatants were subjected to ultracentrifugation to precipitate viral particles, which were then purified by sucrose density gradient centrifugation and dialyzed to remove the sucrose from the viral fraction. After dialysis, the purified viral particles were inactivated by exposure to 0.02% formalin.

Second, eight-week-old female Balb/c mice were injected intraperitoneally with the inactivated purified viral particles at a dose of 3 μg of total protein. The HA content of the purified virus was confirmed to be equivalent by SDS-PAGE (similar mobility and concentrations of the HA protein bands). Eight mice were immunized with each purified viral antigen. Immunization was performed twice at a 3-week interval, and blood samples were obtained 2 weeks after the second dose. Serum samples from the immunized mice were examined by a cross haemagglutination-inhibition (HI) antibody assay with 2 purified viral antigens that were used for immunization as described above [11].

Comparison of the HI antibody titers determined for each individual mouse was done with the unpaired Student's t-test (two-tailed) [12].

3. Results

3.1. Comparison of viral growth and HA titers between egg and cell culture

Table 1 shows the generation of seed viruses by serial culture twice in MDCK cells.

All of the viruses showed efficient replication in these cells during both primary culture and subsequent passages, irrespective of whether they were originally isolated from MDCK cells or eggs. It is noteworthy that the A/Ku M1 virus isolated from MDCK cells showed good growth in MDCK-33016 cells during primary culture as well as in subsequent passages. Even A/Ku E3 and A/Ku E5, which were isolated and passaged in eggs, showed good growth during subsequent passaging in MDCK cells. For pilot culture in eggs, the original viruses were used as the seed.

After pilot culture in MDCK cells and eggs, the HA titers of the culture supernatants and the allantoic fluid and the HA content of partially purified virus were measured. The results are shown in Fig. 2.

When A/Ku M1 virus was cultured in embryonated eggs (A/Ku M1/E1), the virus showed no replication, with no HA titer or HA content of allantoic fluid being detected. Although A/Ku E3 and A/Ku E5 grew in eggs, the yield was lower compared with that for reas-